

CERN-PH-EP/2013-037
2015/01/08

CMS-SMP-12-023

Differential cross section measurements for the production of a W boson in association with jets in proton-proton collisions at $\sqrt{s} = 7$ TeV

The CMS Collaboration*

Abstract

Measurements are reported of differential cross sections for the production of a W boson, which decays into a muon and a neutrino, in association with jets, as a function of several variables, including the transverse momenta (p_T) and pseudorapidities of the four leading jets, the scalar sum of jet transverse momenta (H_T), and the difference in azimuthal angle between the directions of each jet and the muon. The data sample of pp collisions at a centre-of-mass energy of 7 TeV was collected with the CMS detector at the LHC and corresponds to an integrated luminosity of 5.0 fb^{-1} . The measured cross sections are compared to predictions from Monte Carlo generators, MADGRAPH+PYTHIA and SHERPA, and to next-to-leading-order calculations from BLACKHAT+SHERPA. The differential cross sections are found to be in agreement with the predictions, apart from the p_T distributions of the leading jets at high p_T values, the distributions of the H_T at high- H_T and low jet multiplicity, and the distribution of the difference in azimuthal angle between the leading jet and the muon at low values.

Published in Physics Letters B as doi:10.1016/j.physletb.2014.12.003.

1 Introduction

This letter reports measurements of fiducial cross sections for W boson production in association with jets at the LHC. Measurements of the production of vector bosons in association with jets are fundamental tests of perturbative quantum chromodynamics (pQCD). The W+jets processes also provide the main background to other, much rarer, standard model (SM) processes, such as $t\bar{t}$ [1] and single top-quark production [2], and to Higgs boson production and a variety of physics processes beyond the SM. Searches for phenomena beyond the SM are often limited by the uncertainty in the theoretical cross sections for W (and Z) + jets processes at high momentum scales and large jet multiplicities. Therefore, it is crucial to perform precision measurements of W+jets production at the LHC.

Leptonic decay modes of the vector boson are often used in the measurement of SM processes and in searches for new physics, because they provide clean signatures with relatively low background. This letter focuses on the production of a W boson decaying into a muon and a neutrino, as part of a final-state topology characterised by one high-transverse-momentum (p_T) isolated muon, significant missing transverse energy (E_T^{miss}), and one or more jets. The cross sections are measured as a function of the inclusive and exclusive jet multiplicities for up to six jets. Differential cross sections are measured for different inclusive jet multiplicities as a function of the transverse momentum and the pseudorapidity (η) of the jets, where $\eta = -\ln[\tan(\theta/2)]$, and θ is the polar angle measured with respect to the anticlockwise beam direction. The cross sections are also measured as a function of the difference in azimuthal angle between the direction of each jet and that of the muon, and of H_T , which is defined as the scalar sum of the p_T of all jets with $p_T > 30 \text{ GeV}$ and $|\eta| < 2.4$. It is important to study the distribution of the jet p_T and the observable H_T because they are sensitive to higher order corrections, and are often used to discriminate against background in searches for signatures of physics beyond the SM. Additionally, H_T is often used to set the scale of the hard scattering process in theoretical calculations. Finally, the η distributions of jets and the azimuthal separations between the jets and the muon are also important, because they are sensitive to the modelling of parton emission.

The measurements presented in this letter use proton-proton (pp) collision data at a centre-of-mass energy of $\sqrt{s} = 7 \text{ TeV}$ recorded with the CMS detector at the LHC in 2011 and correspond to an integrated luminosity of $5.0 \pm 0.1 \text{ fb}^{-1}$ [3]. These measurements cover high jet multiplicities and higher jet p_T than earlier publications because the centre-of-mass energy and the integrated luminosity are higher. Previous studies of leptonic decay modes of the W boson in association with jets at the LHC have measured the cross sections and cross section ratios for W boson production in association with jets in pp collisions with an integrated luminosity of 36 pb^{-1} at $\sqrt{s} = 7 \text{ TeV}$ with the ATLAS [4] and CMS [5] detectors. Measurements have also been made with $p\bar{p}$ collisions with the D0 detector [6, 7] at the Tevatron collider for integrated luminosities up to 4.2 fb^{-1} , as well as with the CDF detector [8] for an integrated luminosity of 320 pb^{-1} . Recent measurements have been made with the ATLAS detector with a centre-of-mass energy of 7 TeV and an integrated luminosity of 4.6 fb^{-1} [9].

In order to perform a differential measurement of the W+jets cross section, a high-purity sample of $W \rightarrow \mu\nu$ events is selected and the kinematic distributions are corrected to the particle level by means of regularised unfolding [10]. This procedure corrects a measured observable for the effects of detector response, finite experimental resolutions, acceptance, and efficiencies, and therefore allows for direct comparison with theoretical predictions. The measured differential cross sections are compared to the predictions of generators such as MADGRAPH 5.1.1 [11] interfaced with PYTHIA 6.426 [12], SHERPA 1.4.0 [13–16], and BLACKHAT [17, 18], in-

terfaced to SHERPA. The BLACKHAT+SHERPA samples [19] provide parton-level predictions of $W + n$ ($n = 1-5$) jets at next-to-leading order (NLO), while the MADGRAPH+PYTHIA and SHERPA samples provide tree-level calculations followed by hadronisation to produce the final states.

The letter proceeds as follows: Section 2 presents the CMS detector. Section 3 describes the Monte Carlo (MC) event generators, as well as the data samples used for the analysis. The identification criteria for the final-state objects (leptons and jets) and the selection of the $W \rightarrow \mu\nu +$ jets events are presented in Section 4. Section 5 describes the modelling of instrumental backgrounds and irreducible physics backgrounds. The procedure used for unfolding is detailed in Section 6, and Section 7 describes the systematic uncertainties. Finally, the unfolded distributions are presented in Section 8 and compared to theoretical predictions, and Section 9 summarises the results.

2 The CMS detector

The CMS detector, presented in detail elsewhere [20], can be described with a cylindrical coordinate system with the $+z$ axis directed along the anticlockwise beam axis. The detector consists of an inner tracking system and calorimeters (electromagnetic, ECAL, and hadron, HCAL) surrounded by a 3.8 T solenoid. The inner tracking system consists of a silicon pixel and strip tracker, providing the required granularity and precision for the reconstruction of vertices of charged particles in the range $0 \leq \phi < 2\pi$ in azimuth and $|\eta| < 2.5$. The crystal ECAL and the brass/scintillator sampling HCAL are used to measure the energies of photons, electrons, and hadrons within $|\eta| < 3.0$. The HCAL, when combined with the ECAL, measures jets with a resolution $\Delta E/E \approx 100\%/\sqrt{E [\text{GeV}]} \oplus 5\%$ [21]. The three muon systems surrounding the solenoid cover a region $|\eta| < 2.4$ and are composed of drift tubes in the barrel region ($|\eta| < 1.2$), cathode strip chambers in the endcaps ($0.9 < |\eta| < 2.4$), and resistive-plate chambers in both the barrel region and the endcaps ($|\eta| < 1.6$). Events are recorded based on a trigger decision using information from the CMS detector subsystems. The first level (L1) of the CMS trigger system, composed of custom hardware processors, uses information from the calorimeters and muon detectors to select the most interesting events in a fixed time interval of less than $4 \mu\text{s}$. The high-level trigger (HLT) processor further decreases the event rate from 100 kHz at L1 to roughly 300 Hz.

3 Data and simulation samples

Events are retained if they pass a trigger requiring one isolated muon with $p_T > 24 \text{ GeV}$ and $|\eta| < 2.1$. Signal and background simulated samples are produced and fully reconstructed using a simulation of the CMS detector based on GEANT4 [22], and simulated events are required to pass an emulation of the trigger requirements applied to the data. These simulations include multiple collisions in a single bunch crossing (pileup). To model the effect of pileup, minimum bias events generated in PYTHIA are added to the simulated events, with the number of pileup events selected to match the pileup multiplicity distribution observed in data.

A $W \rightarrow \ell\nu + \text{jets}$ signal sample is generated with MADGRAPH 5.1.1 and is used to determine the detector response in the unfolding procedure described in Section 6. Parton showering and hadronisation of the MADGRAPH samples are performed with PYTHIA 6.424 using the Z2 tune [23]. The detector response is also determined using a different $W + \text{jets}$ event sample generated with SHERPA 1.3.0 [13–16], and is used in the evaluation of systematic uncertainties due to the unfolding of the data.

The main sources of background are the production of $t\bar{t}$, single top-quark, Z/γ^* +jets, dibosons ($ZZ/WZ/WW$) + jets, and multijet production. With the exception of multijet production, all backgrounds are estimated from simulation. The simulated samples of $t\bar{t}$ and Z/γ^* +jets are generated with MADGRAPH 5.1.1; single top-quark samples (s -, t -, and tW - channels) are generated with POWHEG version 1.0 [24–27]; VV samples, where V represents either a W boson or a Z boson, are generated with PYTHIA version 6.424 using the Z2 tune [23]. Parton showering and hadronisation of the MADGRAPH and POWHEG samples are performed with PYTHIA 6.424. The simulations with MADGRAPH and PYTHIA use the CTEQ6L1 parton distribution functions (PDF) [28]. The simulation with SHERPA uses the CTEQ6.6m PDF, and the simulations with POWHEG use the CTEQ6m PDF.

The W +jets and Z/γ^* +jets samples are normalised to next-to-next-to-leading order (NNLO) inclusive cross sections calculated with FEWZ [29]. Single top-quark and VV samples are normalised to NLO inclusive cross sections calculated with MCFM [30–33]. The $t\bar{t}$ contribution is normalised to the NNLO + next-to-next-leading logarithm (NNLL) predicted cross section from Ref. [34].

4 Object identification and event selection

Muon candidates are reconstructed as tracks in the muon system that are matched to tracks reconstructed in the inner tracking system [35]. Muon candidates are required to have $p_T > 25$ GeV, and to be reconstructed within the fiducial volume used for the high-level trigger muon selection, i.e. within $|\eta| < 2.1$. This ensures that the offline event selection requirements are as stringent as the trigger. In addition, an isolation requirement is applied to the muon candidates by demanding that the relative isolation is less than 0.15, where the relative isolation is defined as the sum of the transverse energy deposited in the calorimeters (ECAL and HCAL) and of the p_T of charged particles measured with the tracker in a cone of $\Delta R = \sqrt{(\Delta\phi)^2 + (\Delta\eta)^2} = 0.3$ around the muon candidate track (excluding this track), divided by the muon candidate p_T . To ensure a precise measurement of the transverse impact parameter of the muon track relative to the interaction point, only muon candidates with tracks containing more than 10 hits in the silicon tracker and at least one hit in the pixel detector are considered. To reject muons from cosmic rays, the transverse impact parameter of the muon candidate with respect to the primary vertex is required to be less than 2 mm.

Jets are reconstructed using the CMS particle-flow algorithm [36, 37], using the anti- k_T [38, 39] algorithm with a distance parameter of 0.5. The jet energy is calibrated using the p_T balance of dijet and γ +jet events [40] to account for the following effects: nonuniformity and non-linearity of the ECAL and HCAL energy response to neutral hadrons, the presence of extra particles from pileup interactions, the thresholds used in jet constituent selection, reconstruction inefficiencies, and possible biases introduced by the clustering algorithm. Only jets with $p_T > 30$ GeV, $|\eta| < 2.4$, and a spatial separation of $\Delta R > 0.5$ from the muon are considered. To reduce the contamination from pileup jets, jets are required to be associated to the same primary vertex as the muon. The vertex associated to each jet is the one that has the largest number of p_T -weighted tracks in common with the jet. The contamination from pileup jets is estimated with the signal simulation, with pileup events simulated with PYTHIA, and found to be less than 1%.

The missing momentum vector, p_T^{miss} , is defined as the negative of the vectorial sum of the transverse momenta of the particles reconstructed with the particle-flow algorithm, and the E_T^{miss} is defined as the magnitude of the p_T^{miss} vector. The measurement of the E_T^{miss} in simu-

lation is sensitive to the modelling of the calorimeter response and resolution and to the description of the underlying event. To account for these effects, the E_T^{miss} in W+jets simulation is corrected for the differences in the detector response between data and simulation, using a method detailed in Ref. [41]. A recoil energy correction is applied to the W+jets simulation on an event-by-event basis, using a sample of $Z \rightarrow \mu\mu$ events in data and simulation. The transverse recoil vector, defined as the negative vector sum of the missing transverse energy and the transverse momenta of the lepton(s), is divided into components parallel and perpendicular to the boson direction. The mean and the width of the transverse recoil vector components are parameterised as a function of the Z boson p_T in data and simulation. The ratio of the data and simulation parameterisations is used to adjust the transverse recoil vector components in each simulated event, and a new E_T^{miss} is computed using the corrected recoil components.

Events are required to contain exactly one muon satisfying the conditions described above and one or more jets with $p_T > 30 \text{ GeV}$. Events are required to have $M_T > 50 \text{ GeV}$, where M_T , the transverse mass of the muon and missing transverse energy, is defined as $M_T \equiv \sqrt{2p_T^\mu E_T^{\text{miss}} (1 - \cos \Delta\phi)}$, where p_T^μ is the muon p_T and $\Delta\phi$ is the difference in azimuthal angle between the muon momentum direction and the p_T^{miss} vector.

5 Estimation of the backgrounds and selection efficiencies

All background sources except for the multijet production are modelled with simulation. The simulated event samples are corrected for differences between data and simulation in muon identification efficiencies and event trigger efficiency. A “tag-and-probe” method [35] is used to determine the differences between simulation and data for the efficiency of the trigger and for the muon identification and isolation criteria. This method uses $Z \rightarrow \mu\mu$ events from both data and simulated samples where the “tag” muon is required to pass the identification and isolation criteria. The efficiency measurements use the “probe” muon, which is required to pass minimal quality criteria. Trigger efficiency corrections are determined as a function of the muon η , and are in general less than 5%. Muon isolation and identification efficiency corrections are determined as a function of the muon p_T and η , and are generally less than 2%. Corrections to the simulation are applied on an event-by-event basis in the form of event weights.

The dominant background to W+jets production is $t\bar{t}$ production, which has a larger total contribution than that of the W+jets signal in events with four or more jets. In order to reduce the level of $t\bar{t}$ contamination, a veto is applied to events with one or more b-tagged jets. Heavy-flavour tagging is based on a tag algorithm [42] that exploits the long lifetime of b-quark hadrons. This algorithm calculates the signed impact parameter significance of all tracks in the jet that satisfy high-quality reconstruction and purity criteria, and orders the tracks by decreasing significance. The impact parameter significance is defined as the ratio of the impact parameter to its estimated uncertainty. For jets with two or more significant tracks, a high-efficiency b-quark discriminator is defined as the significance of the second most significant track. The size of the $t\bar{t}$ background is illustrated in Fig. 1, before and after the implementation of the b-jet veto, using the event selection described in Section 4. The expected contributions for the different processes in Fig. 1 are shown as a function of the jet multiplicity, along with the observed data. Differences in the tagging and mistagging rates between data and simulation are measured as a function of the jet p_T in multijet and $t\bar{t}$ events [42], and are used to correct the tagging rates of the jets in simulation. For jet multiplicities of 1 to 6, the b-jet veto eliminates 44–84% of the predicted $t\bar{t}$ background, while eliminating 3–26% of the predicted W+jets signal. The resulting increase in the signal purity allows for reductions in the total uncertainty in the measured cross sections of 6–43% for jet multiplicities of 4–6.

The shape and normalisations of the Z/γ^* +jets and $t\bar{t}$ predictions are cross-checked in selected data samples. The Z +jets background is compared to data in a Z -boson dominated data sample that requires two well-identified, isolated muons. The $t\bar{t}$ background is compared to data in a control region requiring at least two b -tagged jets. Background estimations from simulation and from data control samples agree within the uncertainties described in Section 7.

The multijet background is estimated using a data control sample with an inverted muon isolation requirement. In the control sample, the muon misidentification rate for multijet processes is estimated in the multijet-enriched sideband region with $M_T < 50$ GeV, and the shape template of the multijet distribution is determined in the region with $M_T > 50$ GeV. Contributions from other processes to the multijet control region are subtracted, including the dominant contribution from W +jets. In order to improve the estimation of W +jets in the multijet control region, the W +jets contribution is first normalised to data in the $M_T > 50$ GeV region with the muon isolation condition applied. The multijet shape template is then rescaled according to the muon misidentification rate. For exclusive jet multiplicities of 1–4, the purity of the multijet-enriched inverted-isolation sideband region is 99.7–98.1%, and the purity of the W +jets contribution to the signal region is 92–76%. The multijet estimate corresponds to 32.7–1.9% of the total background estimate, or 2.6–0.3% of the total SM prediction.

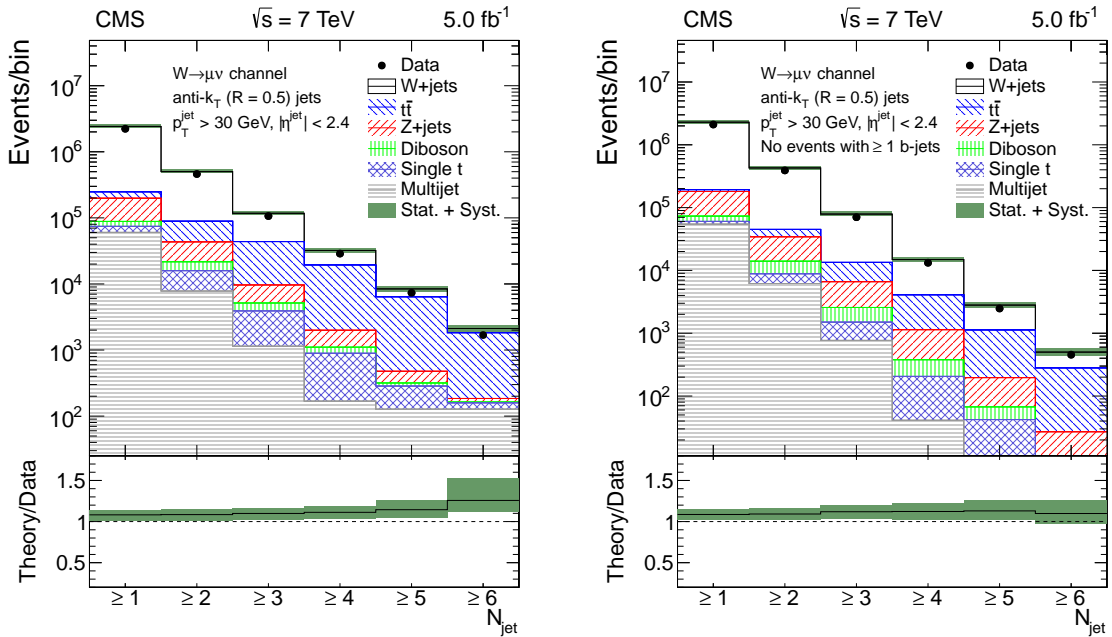


Figure 1: The jet multiplicity in data and simulation before (left) and after (right) the b -jet veto. The W +jets contribution is modelled with MADGRAPH 5.1.1+PYTHIA 6.424. The solid band indicates the total statistical and systematic uncertainty in the W +jets signal and background predictions, as detailed in Section 7. This includes uncertainties in the jet energy scale and resolution, the muon momentum scale and resolution, the pileup modelling, the b -tagging correction factors, the normalisations of the simulations, and the efficiencies of reconstruction, identification, and trigger acceptance. A substantial reduction in the expected $t\bar{t}$ background is observed in the right plot.

6 The unfolding procedure

For the measurement of cross sections, the particle level is defined by a W boson, which decays into a muon and a muon neutrino, produced in association with one or more jets. Kinematic thresholds on the particle-level muon, M_T , and jets are identical to those applied to the reconstructed objects. Specifically, the particle-level selection includes the requirement of exactly one muon with $p_T > 25$ GeV and $|\eta| < 2.1$, and $M_T > 50$ GeV. The particle-level E_T^{miss} is defined as the negative of the vectorial sum of the transverse momenta of all visible final state particles. To account for final-state radiation, the momenta of all photons in a cone of $\Delta R < 0.1$ around the muon are added to that of the muon. Jets are clustered using the anti- k_T [38] algorithm with a distance parameter of 0.5. Clustering is performed using all particles after decay and fragmentation, excluding neutrinos and the muon from the W boson decay. Additionally, jets are required to have $p_T > 30$ GeV and $|\eta| < 2.4$, and to be separated from the muon by $\Delta R > 0.5$.

The reconstructed distributions are corrected to the particle level with the method of regularised singular value decomposition (SVD) [10] unfolding, using the ROOUNFOLD toolkit [43]. For each distribution, the total background, including the multijet estimate from data and all simulated processes except the W boson signal, is subtracted from the data before unfolding. A response matrix, defining the migration probability between the particle-level and reconstructed quantities, as well as the overall reconstruction efficiency, is computed using W +jets events simulated with MADGRAPH+PYTHIA. For a given particle-level quantity Q with a corresponding reconstructed quantity Q' , the migration probability from an interval $a < Q < b$ to an interval $c < Q' < d$ is defined as the fraction of events with $a < Q < b$ that have $c < Q' < d$. The unfolding of the jet multiplicity is performed with a response defined by the number of particle-level jets versus the number of reconstructed jets. For particle-level jet multiplicities of 1 to 6, 4 to 51% of simulated events exhibit migration to different values of reconstructed jet multiplicity. The unfolding of the kinematic distributions of the n th jet is performed with a response defined by the kinematic quantity of the n th-highest- p_T particle-level jet versus that of the n th-highest- p_T reconstructed jet. To achieve a full migration from the selection of reconstructed events to the particle-level phase space, no matching between reconstructed and particle-level jets is applied. The contribution from the $W \rightarrow \tau\nu$ process with a muon in the final state is estimated to be at the 1% level, and is not considered as part of the signal definition at the particle level.

The b-jet veto is treated as an overall event selection condition. Events failing this condition are treated as nonreconstructed in the unfolding response, so that the cross section obtained after unfolding is valid for W boson decays with associated jets of any flavour.

7 Systematic uncertainties

The sources of systematic uncertainties considered in this analysis are described below. The entirety of the unfolding procedure is repeated for each systematic variation, and the unfolded data results with these variations are compared with the central (unvaried) results to extract the uncertainties in the unfolded data distributions.

In most distributions, the dominant sources of systematic uncertainty include the jet energy scale and resolution uncertainties, which affect the shape of all reconstructed distributions as well as the overall event acceptance. The jet energy scale uncertainties are estimated by assigning a p_T - and η -dependent uncertainty in jet energy corrections as discussed in Ref. [40], and by varying the jet p_T by the magnitude of the uncertainty. The uncertainties in jet energy resolution are assessed by increasing the p_T difference between the reconstructed and particle-level

jets by an η -dependent value [40]. The jet energy uncertainties are determined by varying the p_T of the jets in data rather than in simulation.

Muon momentum scale and resolution uncertainties also introduce uncertainties in the overall event acceptance. A muon momentum scale uncertainty of 0.2% and a muon momentum resolution uncertainty of 0.6% are assumed [35]. The effects of these uncertainties are assessed by directly varying the momentum scale and randomly fluctuating the muon momentum in the simulation.

Variations for uncertainties in the energy and momentum scales and resolutions affect the size and shape of the background distribution to be subtracted from the data distribution, as well as the acceptance of W +jets simulated events, which define the response matrix used for unfolding. The variations are also propagated to the measurement of E_T^{miss} , which affects the acceptance of the $M_T > 50$ GeV requirement.

Another important source of systematic uncertainty is the choice of the generator used in the unfolding procedure. The size of this uncertainty is assessed by repeating the unfolding procedure with a response trained on a separate simulated sample generated with SHERPA 1.3.0. The absolute value of the difference between the data unfolded with a response matrix trained on SHERPA and with a response matrix trained on MADGRAPH+PYTHIA is treated as a symmetric uncertainty in the measurement.

Other minor sources of systematic uncertainty include the uncertainties in the background normalisation, the b -tagging efficiency, the modelling of the Wb contribution in the signal simulation, integrated luminosity, the pileup modelling, the trigger and object identification efficiencies, and the finite number of simulated events used to construct the response matrix. Background normalisation uncertainties are determined by varying the cross sections of the backgrounds within their theoretical uncertainties. For the Z +jets process, a normalisation uncertainty of 4.3% is calculated as the sum in quadrature of the factorisation/renormalisation scale and PDF uncertainties calculated in FEWZ [29]. For the diboson and single top-quark processes, uncertainties are calculated with MCFM [30–33] to be 4% and 6%, respectively. The uncertainty in the $t\bar{t}$ modelling is assessed by taking the difference between data and simulation in a control region with two or more b -tagged jets, and is estimated to be 5 to 12% for jet multiplicities of 2 to 6. The estimate of the multijet background has an uncertainty based on the limited number of events in the multijet sample and in the control regions where the multijet sample normalisation is calculated, and other systematic variations affecting the backgrounds in the multijet control regions introduce variations in the multijet normalization and template shape. For the b -tagging algorithm used to veto events containing b jets, uncertainties in the data/simulation ratio of the b -tagging efficiencies are applied. For jets with $p_T > 30$ GeV, these uncertainties range from 3.1 to 10.5%. An additional uncertainty is ascribed to the normalisation of the Wb content in the simulation by examining the agreement between data and simulation as a function of jet multiplicity in a control region defined by requiring exactly one b -tagged jet. An increase in the normalisation of the Wb process of 120% is considered, yielding an uncertainty in the measurement of 0.5 to 11% for jet multiplicities of 1 to 6. The uncertainty in the integrated luminosity is 2.2% [3]. An uncertainty in the modelling of pileup in simulation is determined by varying the number of simulated pileup interactions by 5% to account for the uncertainty in the luminosity and the uncertainty in the total inelastic cross section [44], as determined by a comparison of the number of reconstructed vertices in $Z \rightarrow \mu\mu$ events in data and simulation. Uncertainties in the differences between data and simulation efficiencies of the trigger, muon isolation, and muon identification criteria are generally less than 1%. An additional uncertainty due to the finite number of simulated events used to construct the re-

sponse matrix is calculated by randomly varying the content of the response matrix according to a Poisson uncertainty in each bin.

The effect of the systematic variations on the measured cross section as a function of the exclusive jet multiplicity is illustrated in Fig. 2. The uncertainties given in Fig. 2 are the total uncertainty for each jet multiplicity. The corresponding ranges of systematic uncertainty across bins of jet p_T are given in Table 1.

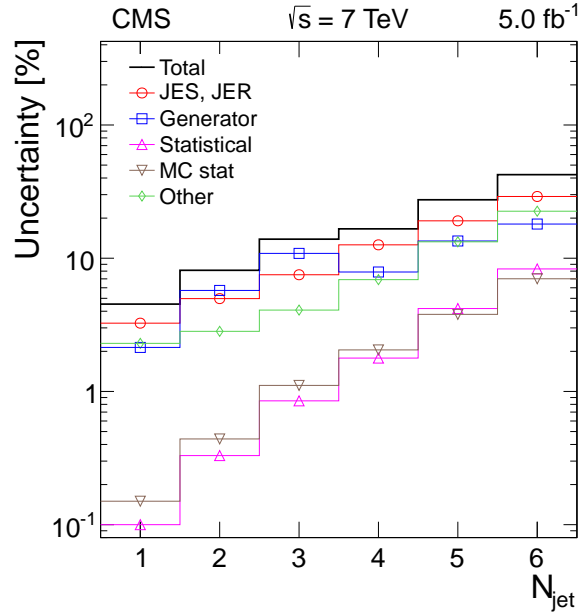


Figure 2: The dominant systematic uncertainties in the measurement of the W+jets cross section as a function of the exclusive jet multiplicity. The systematic uncertainties displayed include the jet energy scale and resolution (JES, JER), the choice of generator used in the unfolding procedure (Generator), the statistical uncertainty in the data minus the background, propagated through the unfolding procedure (Statistical), the uncertainty due to a finite number of simulated events used to construct the response matrix (MC stat.), and all other systematic uncertainties (Other) detailed in Section 7, including pileup, integrated luminosity, background normalisation, b-tagging, muon momentum and resolution, trigger efficiency, muon identification. The uncertainties presented here correspond to the weighted average of the values shown in Table 1.

8 Results

The cross sections for exclusive and inclusive jet multiplicities are given in Fig. 3. In Figs. 4–7 the differential cross sections are presented. The measured W+jets cross sections are compared to the predictions from several generators. We consider W+jets signal processes generated with MADGRAPH 5.1.1 using the CTEQ6L1 PDF set, with SHERPA 1.4.0 using the CT10 [45, 46] PDF set, and with BLACKHAT+SHERPA [17] using the CT10 PDF set. Predictions from MADGRAPH +PYTHIA and SHERPA are normalised to the NNLO inclusive cross sections calculated with FEWZ [29]. The SHERPA sample is a separate sample from that used for the evaluation of uncertainties in Section 7. The MADGRAPH and SHERPA predictions provide leading-order (LO) matrix element (ME) calculations at each jet multiplicity, which are then combined into inclusive samples by matching the ME partons to particle jets. Parton showering (PS) and hadronisation of the MADGRAPH sample is performed with PYTHIA 6.426 using the Z2 tune.

Table 1: Ranges of uncertainties for the measurement of $d\sigma/dp_T$ of the n th jet in events with n or more jets. The uncertainties displayed include the statistical uncertainty in the data minus the background, propagated through the unfolding procedure (Statistical), the jet energy scale and resolution (JES, JER), the choice of generator used in the unfolding procedure (Generator), the uncertainty due to a finite number of simulated events used to construct the response matrix (MC stat.), and all other systematic uncertainties (Other) detailed in Section 7, including pileup, integrated luminosity, background normalisation, b-tagging, muon momentum and resolution, trigger efficiency, muon identification.

n	p_T [GeV]	Statistical [%]	JES, JER [%]	Generator [%]	MC stat. [%]	Other [%]	Total [%]
1	30–850	0.1–3.2	3.4–24	0.9–9.6	0.2–11	2.3–6.6	4.5–29
2	30–550	0.4–2.4	4.6–12	1.6–13	0.8–11	2.9–5.9	6.9–21
3	30–450	0.6–16	6.0–23	2.7–48	1.0–45	4.5–11	9.4–73
4	30–210	1.6–10	11–15	6.4–21	2.4–23	7.2–26	16–43

The MADGRAPH+PYTHIA calculation includes the production of up to four partons. The jet matching is performed following the k_T -MLM prescription [47], where partons are clustered using the k_T algorithm with a distance parameter of $D = 1$. The k_T clustering thresholds are chosen to be 10 GeV and 20 GeV at the matrix-element and parton-shower level, respectively. The factorisation scale for each event is chosen to be the transverse mass computed after k_T -clustering of the event down to a $2 \rightarrow 2$ topology. The renormalisation scale for the event is the k_T computed at each vertex splitting. The predictions from SHERPA include the production of up to four partons. The matching between jets and partons is performed with the CKKW matching scheme [47], and the default factorisation and renormalisation scales are used.

The predictions from MADGRAPH+PYTHIA and SHERPA are shown with statistical uncertainties only. These MADGRAPH+PYTHIA and SHERPA samples are processed through the RIVET toolkit [48] in order to create particle level distributions, which can be compared with the unfolded data. The BLACKHAT+SHERPA samples represent fixed-order predictions at the level of ME partons of $W + n$ jets at NLO accuracy, for $n = 1, 2, 3, 4$, and 5 jets. Each measured distribution for a given inclusive jet multiplicity is compared with the corresponding fixed-order prediction from BLACKHAT+SHERPA. The choice of renormalisation and factorisation scales for BLACKHAT+SHERPA is $\hat{H}'_T/2$, where $\hat{H}'_T \equiv \sum_m p_T^m + E_T^W$, m represents the final state partons, and E_T^W is the transverse energy of the W boson. Before comparing to data, a nonperturbative correction is applied to the BLACKHAT+SHERPA distributions to account for the effects of multiple-parton interactions and hadronisation. The nonperturbative correction is determined using MADGRAPH 5.1.1 interfaced to PYTHIA 6.426 and turning on and off the hadronisation and multiple-parton interactions. The magnitude of the nonperturbative correction is typically 1–5%, and is calculated for each bin of each measured distribution. The model dependence of the nonperturbative correction is negligible [49]. The BLACKHAT+SHERPA prediction also includes uncertainties due to the PDF and variations of the factorisation and renormalisation scales. The nominal prediction is given by the central value of the CT10 PDF set, and the PDF uncertainty considers the envelope of the error sets of CT10, MSTW2008nlo68cl [50], and NNPDF2.1 [51] according to the PDF4LHC prescription [52, 53]. The factorisation and renormalisation scale uncertainty is determined by varying the scales simultaneously by a factor 0.5 or 2.0.

The unfolded exclusive and inclusive jet multiplicity distributions, shown in Fig. 3, are found to be in agreement, within uncertainties, with the predictions of the generators and with the NLO calculation of BLACKHAT+SHERPA. Table 2 details the measured cross sections as a function of the inclusive and exclusive jet multiplicity.

The jet p_T unfolded distributions for inclusive jet multiplicities from 1 to 4 are shown in Fig. 4. The predictions of BLACKHAT+SHERPA are in agreement with the measured distributions within the systematic uncertainties, while MADGRAPH+PYTHIA is observed to overestimate the yields up to 50% (45%) for the first (second) leading jet p_T distributions at high- p_T values. The predictions from SHERPA are found to agree well for the second-, third-, and fourth-leading jet p_T distributions, while an excess of slightly more than one standard deviation can be seen at high- p_T values for the leading jet p_T distribution. Similar observations hold for MADGRAPH+PYTHIA and SHERPA predictions in the H_T distributions for inclusive jet multiplicities of 1–4, as shown in Fig. 5. Since the BLACKHAT+SHERPA NLO prediction for $H_T(\geq 1 \text{ jet})$ is a fixed-order prediction with up to two real partons, contributions from higher jet multiplicities are missing, which results in an underestimation in the tail of the distribution [54]. Similar observations have been made with W+jets measurements at D0 [7] and ATLAS [4]. In general, SHERPA models the H_T distributions better than other generators.

The distributions of the jet η and of the difference in azimuthal angle between each jet and the muon are shown in Figs. 6 and 7, respectively. The measurements of the jet η agree with predictions from all generators, with MADGRAPH+PYTHIA and BLACKHAT+SHERPA performing best. The measurements of the $\Delta\phi$ between the leading jet and the muon are underestimated by as much as 38% by BLACKHAT+SHERPA, with similar, but smaller, underestimations in predictions from MADGRAPH+PYTHIA and SHERPA.

Examples of the variation in the BLACKHAT+SHERPA prediction due to the choice of PDF are given in Fig. 8, in which the predictions with the MSTW2008nlo68cl, NNPDF2.1, and CT10 PDF sets are compared to the measurements from data. The distributions determined with the different PDF sets are consistent with one another.

Table 2: Cross section measurements with statistical and systematic uncertainties for inclusive and exclusive jet multiplicities up to 6 jets.

Jet multiplicity	Exclusive σ [pb]	Inclusive σ [pb]
1	384^{+15}_{-17}	480^{+18}_{-20}
2	$79.1^{+6.2}_{-5.9}$	$95.6^{+8.5}_{-8.0}$
3	$13.6^{+1.9}_{-1.6}$	$16.6^{+2.3}_{-2.0}$
4	$2.48^{+0.40}_{-0.36}$	$2.93^{+0.52}_{-0.48}$
5	$0.382^{+0.097}_{-0.097}$	$0.45^{+0.12}_{-0.12}$
6	$0.056^{+0.020}_{-0.022}$	$0.067^{+0.023}_{-0.026}$

9 Summary

Measurements of the cross sections and differential cross sections for a W boson produced in association with jets in pp collisions at a centre-of-mass energy of 7 TeV have been presented. The data were collected with the CMS detector during the 2011 pp run of the LHC, and correspond to an integrated luminosity of 5.0 fb^{-1} . Cross sections have been determined using the muon decay mode of the W boson and were presented as functions of the jet multiplicity, the transverse momenta and pseudorapidities of the four leading jets, the difference in azimuthal angle between each jet and the muon, and the H_T for jet multiplicities up to four. The results, corrected for all detector effects by means of regularised unfolding, have been compared with particle-level simulated predictions from pQCD.

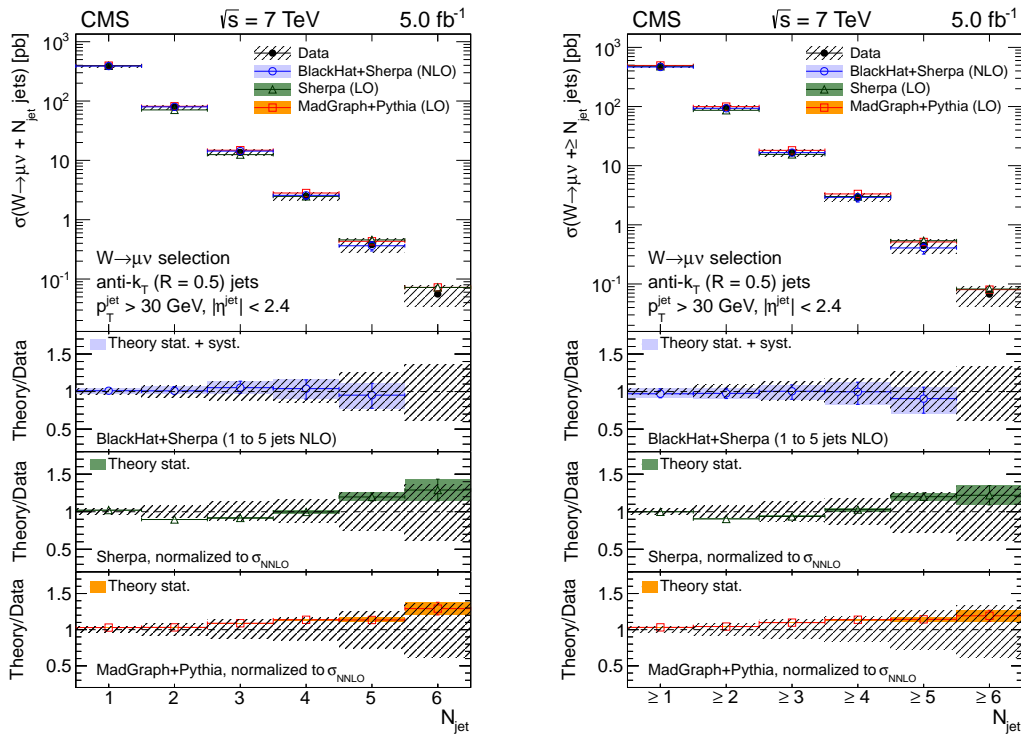


Figure 3: The cross section measurement for the exclusive and inclusive jet multiplicities, compared to the predictions of MADGRAPH 5.1.1 + PYTHIA 6.426, SHERPA 1.4.0, and BLACKHAT+SHERPA (corrected for hadronisation and multiple-parton interactions). Black circular markers with the grey hatched band represent the unfolded data measurement and its uncertainty. Overlaid are the predictions together with their statistical uncertainties (Theory stat.). The BLACKHAT+SHERPA uncertainty also contains theoretical systematic uncertainties (Theory syst.) described in Section 8. The lower plots show the ratio of each prediction to the unfolded data.

Predictions from generators, MADGRAPH+PYTHIA and SHERPA, and NLO calculations from BLACKHAT+SHERPA, describe the jet multiplicity within the uncertainties. The cross section as a function of the p_T of the leading jet is overestimated by MADGRAPH+PYTHIA and SHERPA, especially at high- p_T . Some overestimation from MADGRAPH+PYTHIA can also be observed in the second- and third-leading jet p_T distributions. The cross sections as a function of p_T predicted by BLACKHAT+SHERPA agree with the measurements within uncertainties. The predictions from BLACKHAT+SHERPA underestimate the measurement of the cross section as a function of H_T for $N_{\text{jet}} \geq 1$, since the contribution from $W+\geq 3$ jets is missing from an NLO prediction of $W+\geq 1$ jet. The cross sections as a function of H_T for $N_{\text{jet}} \geq 2, 3$, and 4 predicted by BLACKHAT+SHERPA agree with the measurements within the uncertainties. The distributions of $\Delta\phi$ between the leading jet and the muon are underestimated by all predictions for $\Delta\phi$ values near zero, with the largest disagreement visible in BLACKHAT+SHERPA. The distributions of $\Delta\phi$ between the second-, third-, and fourth-leading jets and the muon agree with all predictions within uncertainties. No significant disagreement was found in the distributions of η of the four leading jets.

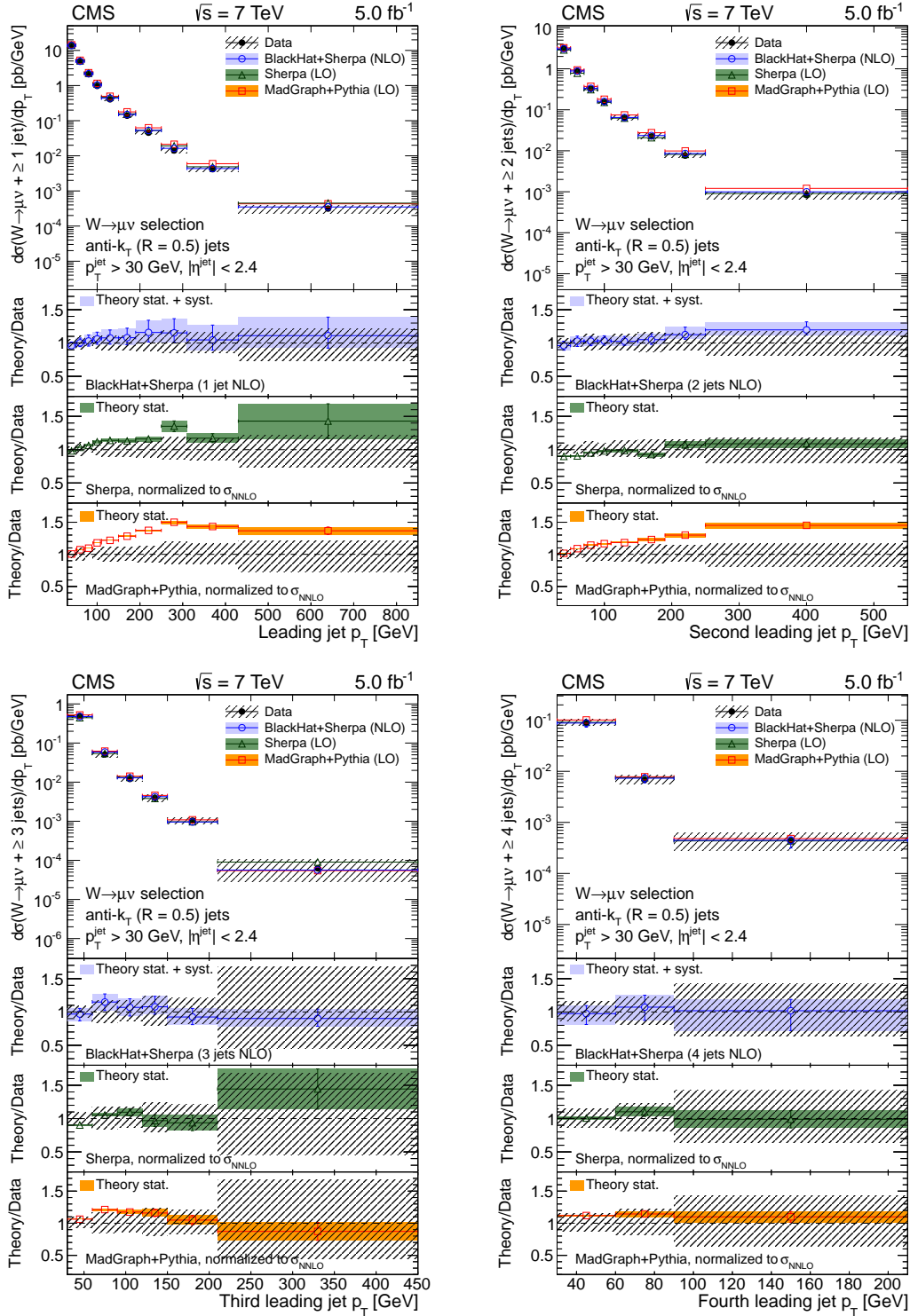


Figure 4: The differential cross section measurement for the leading four jets' transverse momenta, compared to the predictions of MADGRAPH 5.1.1 + PYTHIA 6.426, SHERPA 1.4.0, and BLACKHAT+SHERPA (corrected for hadronisation and multiple-parton interactions). Black circular markers with the grey hatched band represent the unfolded data measurement and its uncertainty. Overlaid are the predictions together with their statistical uncertainties (Theory stat.). The BLACKHAT+SHERPA uncertainty also contains theoretical systematic uncertainties (Theory syst.) described in Section 8. The lower plots show the ratio of each prediction to the unfolded data.

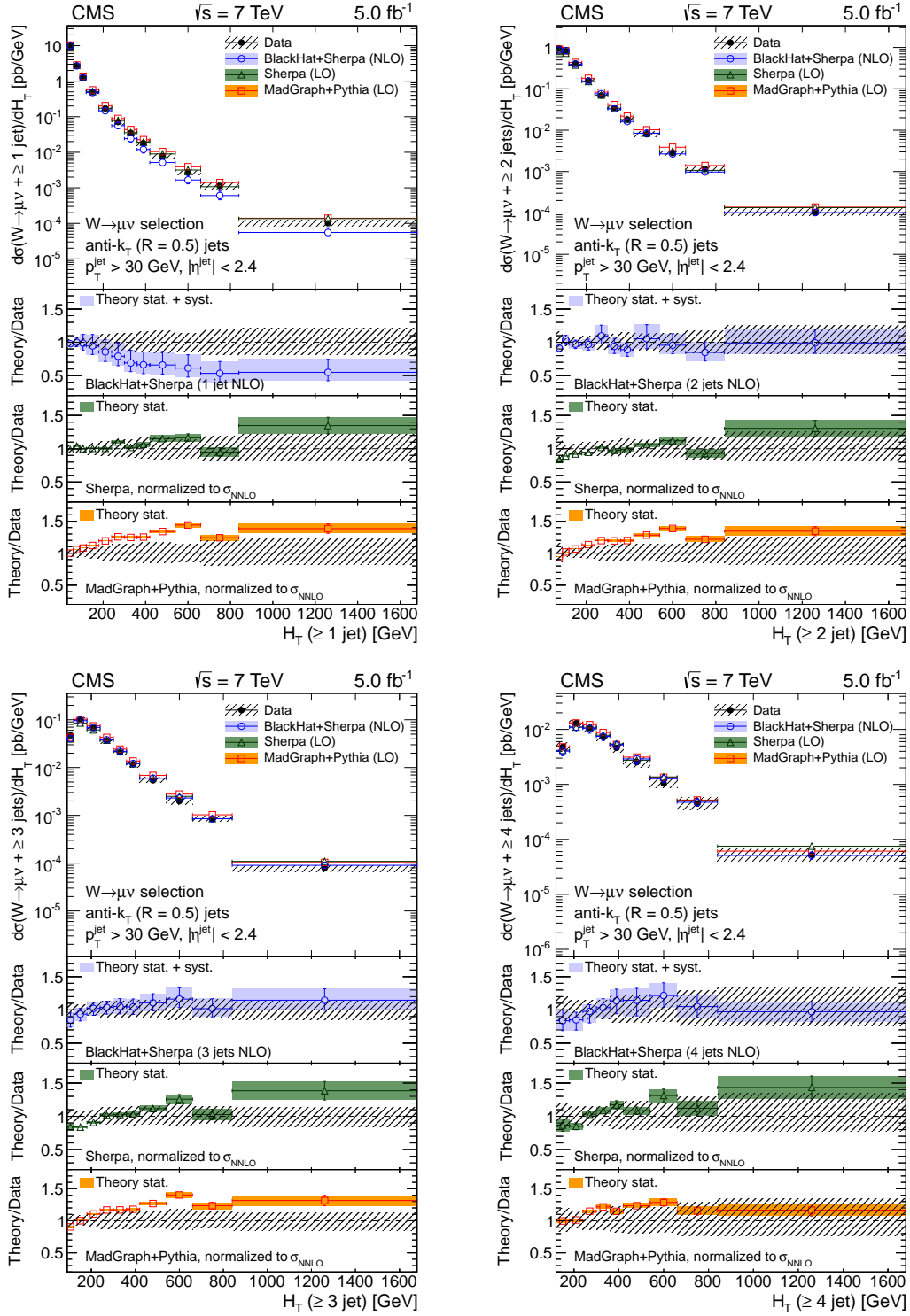


Figure 5: The differential cross section measurement for H_T for inclusive jet multiplicities 1–4, compared to the predictions of MADGRAPH 5.1.1 + PYTHIA 6.426, SHERPA 1.4.0, and BLACKHAT+SHERPA (corrected for hadronisation and multiple-parton interactions). Black circular markers with the grey hatched band represent the unfolded data measurement and its uncertainty. Overlaid are the predictions together with their statistical uncertainties (Theory stat.). The BLACKHAT+SHERPA uncertainty also contains theoretical systematic uncertainties (Theory syst.) described in Section 8. The lower plots show the ratio of each prediction to the unfolded data.

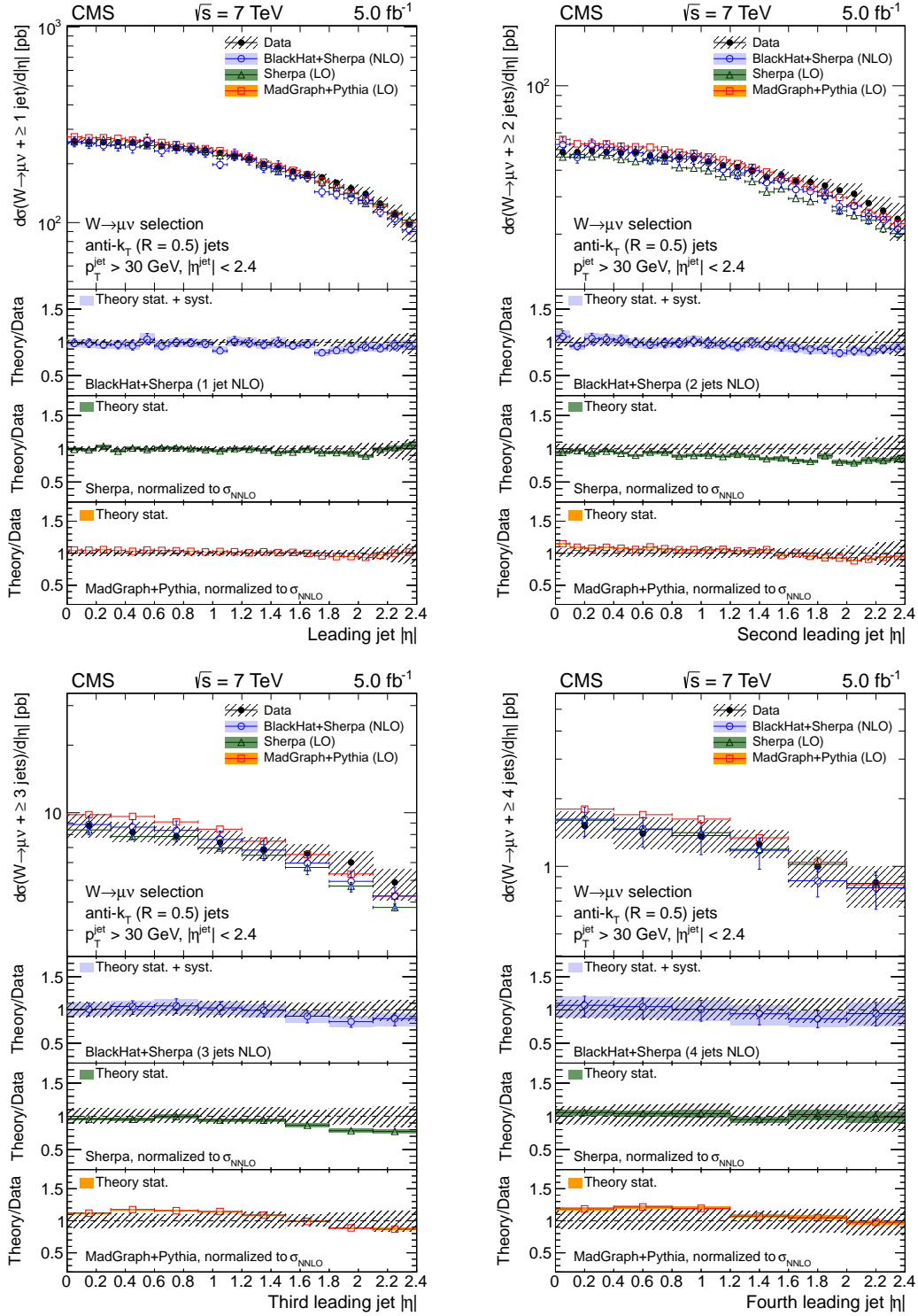


Figure 6: The differential cross section measurement for the pseudorapidity of the four leading jets, compared to the predictions of MADGRAPH 5.1.1 + PYTHIA 6.426, SHERPA 1.4.0, and BLACKHAT+SHERPA (corrected for hadronisation and multiple-parton interactions). Black circular markers with the grey hatched band represent the unfolded data measurement and its uncertainty. Overlaid are the predictions together with their statistical uncertainties (Theory stat.). The BLACKHAT+SHERPA uncertainty also contains theoretical systematic uncertainties (Theory syst.) described in Section 8. The lower plots show the ratio of each prediction to the unfolded data.

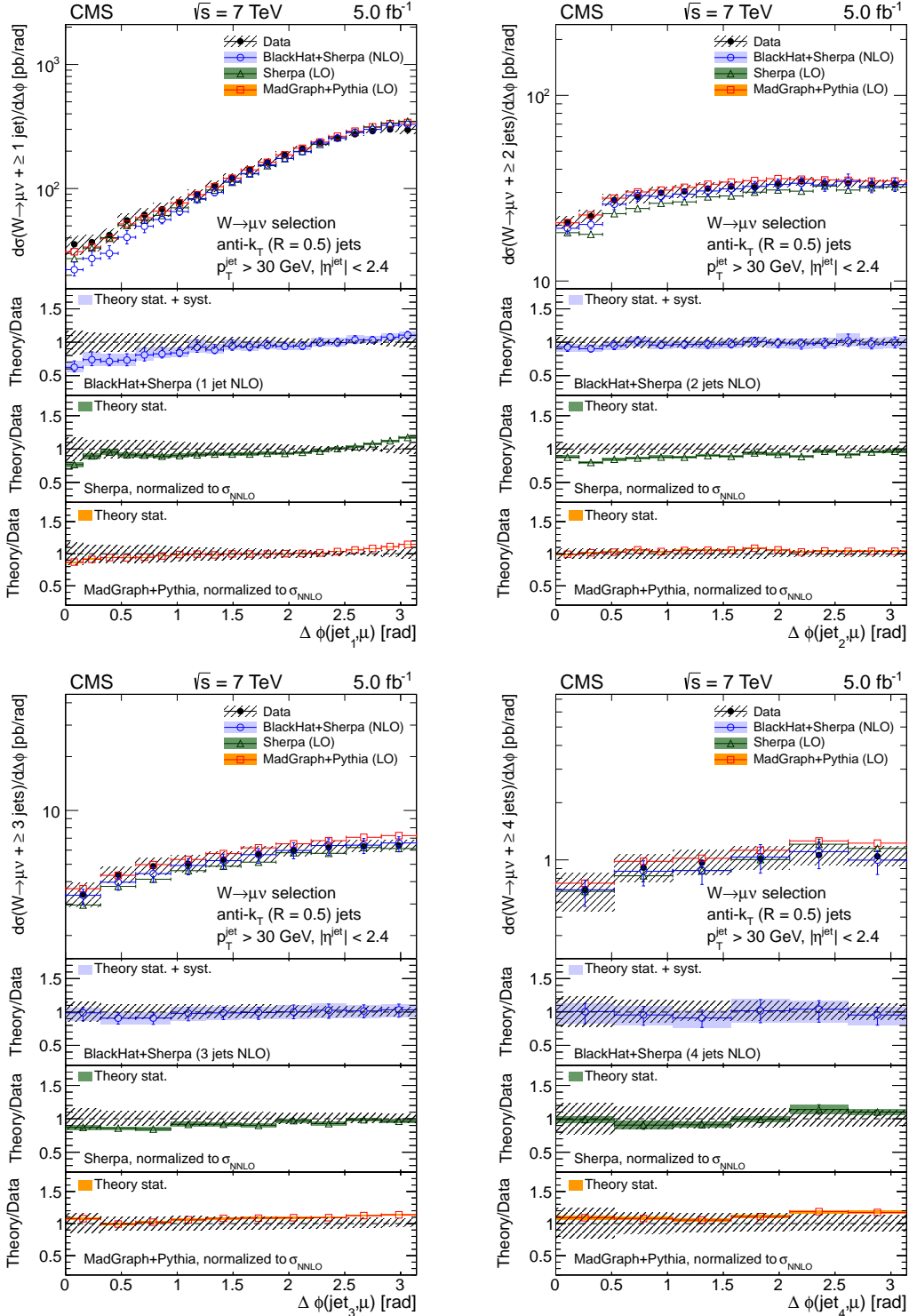


Figure 7: The differential cross section measurement in $\Delta\phi(\text{jet}_n, \mu)$, for $n = 1 - 4$, compared to the predictions of MADGRAPH 5.1.1 + PYTHIA 6.426, SHERPA 1.4.0, and BLACKHAT+SHERPA (corrected for hadronisation and multiple-parton interactions). Black circular markers with the grey hatched band represent the unfolded data measurement and its uncertainty. Overlaid are the predictions together with their statistical uncertainties (Theory stat.). The BLACKHAT+SHERPA uncertainty also contains theoretical systematic uncertainties (Theory syst.) described in Section 8. The lower plots show the ratio of each prediction to the unfolded data.

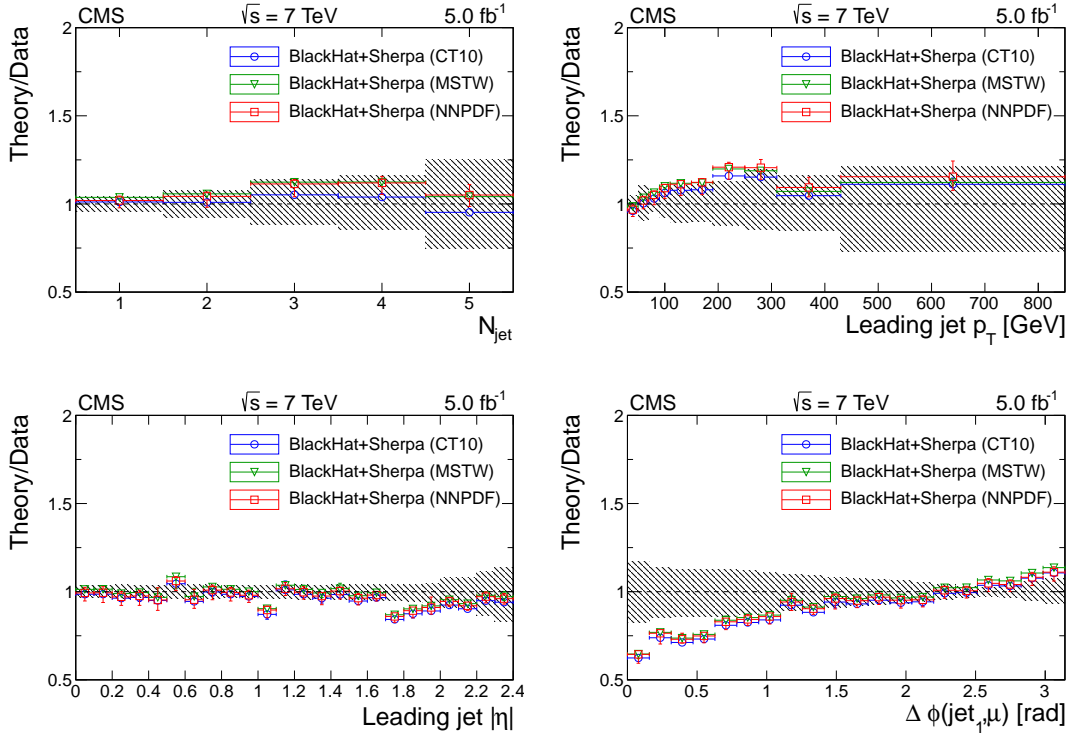


Figure 8: The ratio of the predictions of BLACKHAT+SHERPA to the cross section measurements for four different quantities. The circular, triangular, and square markers indicate the predictions using the CT10, MSTW2008nlo68cl, and NNPDF PDF sets, respectively. The grey hatched band indicates the total uncertainty in the unfolded data measurement.

Acknowledgments

We extend our thanks to Daniel Maître and Zvi Bern for the production of data and tools used to create the BLACKHAT+SHERPA predictions, and for the sharing of expertise and advice regarding these predictions.

We congratulate our colleagues in the CERN accelerator departments for the excellent performance of the LHC and thank the technical and administrative staffs at CERN and at other CMS institutes for their contributions to the success of the CMS effort. In addition, we gratefully acknowledge the computing centres and personnel of the Worldwide LHC Computing Grid for delivering so effectively the computing infrastructure essential to our analyses. Finally, we acknowledge the enduring support for the construction and operation of the LHC and the CMS detector provided by the following funding agencies: BMWFW and FWF (Austria); FNRS and FWO (Belgium); CNPq, CAPES, FAPERJ, and FAPESP (Brazil); MES (Bulgaria); CERN; CAS, MoST, and NSFC (China); COLCIENCIAS (Colombia); MSES and CSF (Croatia); RPF (Cyprus); MoER, ERC IUT and ERDF (Estonia); Academy of Finland, MEC, and HIP (Finland); CEA and CNRS/IN2P3 (France); BMBF, DFG, and HGF (Germany); GSRT (Greece); OTKA and NIH (Hungary); DAE and DST (India); IPM (Iran); SFI (Ireland); INFN (Italy); NRF and WCU (Republic of Korea); LAS (Lithuania); MOE and UM (Malaysia); CINVESTAV, CONACYT, SEP, and UASLP-FAI (Mexico); MBIE (New Zealand); PAEC (Pakistan); MSHE and NSC (Poland); FCT (Portugal); JINR (Dubna); MON, RosAtom, RAS and RFBR (Russia); MESTD (Serbia); SEIDI and CPAN (Spain); Swiss Funding Agencies (Switzerland); MST (Taipei); ThEPCenter, IPST, STAR and NSTDA (Thailand); TUBITAK and TAEK (Turkey); NASU and SFFR (Ukraine); STFC (United Kingdom); DOE and NSF (USA).

Individuals have received support from the Marie-Curie programme and the European Research Council and EPLANET (European Union); the Leventis Foundation; the A. P. Sloan Foundation; the Alexander von Humboldt Foundation; the Belgian Federal Science Policy Office; the Fonds pour la Formation à la Recherche dans l'Industrie et dans l'Agriculture (FRIA-Belgium); the Agentschap voor Innovatie door Wetenschap en Technologie (IWT-Belgium); the Ministry of Education, Youth and Sports (MEYS) of the Czech Republic; the Council of Science and Industrial Research, India; the HOMING PLUS programme of Foundation for Polish Science, cofinanced from European Union, Regional Development Fund; the Compagnia di San Paolo (Torino); the Thalís and Aristeia programmes cofinanced by EU-ESF and the Greek NSRF; and the National Priorities Research Program by Qatar National Research Fund.

References

- [1] CMS Collaboration, "Measurement of the $t\bar{t}$ production cross section in pp collisions at $\sqrt{s} = 7$ TeV with lepton + jets final states", *Phys. Lett. B* **720** (2012) 83, doi:10.1016/j.physletb.2013.02.021, arXiv:1212.6682.
- [2] CMS Collaboration, "Measurement of the single-top-quark t -channel cross section in pp collisions at $\sqrt{s} = 7$ TeV", *JHEP* **12** (2012) 035, doi:10.1007/JHEP12(2012)035, arXiv:1209.4533.
- [3] CMS Collaboration, "Absolute Calibration of the Luminosity Measurement at CMS: Winter 2012 Update", CMS Physics Analysis Summary CMS-PAS-SMP-12-008, 2012.
- [4] ATLAS Collaboration, "Study of jets produced in association with a W boson in pp collisions at $\sqrt{s} = 7$ TeV with the ATLAS detector", *Phys. Rev. D* **85** (2012) 092002, doi:10.1103/PhysRevD.85.092002, arXiv:1201.1276.
- [5] CMS Collaboration, "Jet production rates in association with W and Z bosons in pp collisions at $\sqrt{s} = 7$ TeV", *JHEP* **01** (2012) 010, doi:10.1007/JHEP01(2012)010, arXiv:1110.3226.
- [6] D0 Collaboration, "Measurements of inclusive W +jets production rates as a function of jet transverse momentum in $p\bar{p}$ collisions at $\sqrt{s} = 1.96$ TeV", *Phys. Lett. B* **705** (2011) 200, doi:10.1016/j.physletb.2011.10.011, arXiv:1106.1457.
- [7] D0 Collaboration, "Studies of W boson plus jets production in $p\bar{p}$ collisions at $\sqrt{s} = 1.96$ TeV", *Phys. Rev. D* **88** (2013) 092001, doi:10.1103/PhysRevD.88.092001, arXiv:1302.6508.
- [8] CDF Collaboration, "Measurement of the cross section for W -boson production in association with jets in $p\bar{p}$ collisions at $\sqrt{s} = 1.96$ TeV", *Phys. Rev. D* **77** (2008) 011108, doi:10.1103/PhysRevD.77.011108, arXiv:0711.4044.
- [9] ATLAS Collaboration, "Measurements of the W production cross sections in association with jets with the ATLAS detector", (2014). arXiv:1409.8639.
- [10] A. Hocker and V. Kartvelishvili, "SVD approach to data unfolding", *Nucl. Instrum. Meth. A* **372** (1996) 469, doi:10.1016/0168-9002(95)01478-0, arXiv:hep-ph/9509307.

- [11] J. Alwall et al., “MadGraph 5: going beyond”, *JHEP* **06** (2011) 128, doi:10.1007/JHEP06(2011)128, arXiv:1106.0522.
- [12] T. Sjostrand, S. Mrenna, and P. Skands, “PYTHIA 6.4 physics and manual”, *JHEP* **05** (2006) 026, doi:10.1088/1126-6708/2006/05/026, arXiv:hep-ph/0603175.
- [13] T. Gleisberg and S. Höche, “Comix, a new matrix element generator”, *JHEP* **12** (2008) 039, doi:10.1088/1126-6708/2008/12/039, arXiv:0808.3674.
- [14] S. Schumann and F. Krauss, “A parton shower algorithm based on Catani-Seymour dipole factorisation”, *JHEP* **03** (2008) 038, doi:10.1088/1126-6708/2008/03/038, arXiv:0709.1027.
- [15] T. Gleisberg et al., “Event generation with SHERPA 1.1”, *JHEP* **02** (2009) 007, doi:10.1088/1126-6708/2009/02/007, arXiv:0811.4622.
- [16] S. Höche, F. Krauss, S. Schumann, and F. Siegert, “QCD matrix elements and truncated showers”, *JHEP* **05** (2009) 053, doi:10.1088/1126-6708/2009/05/053, arXiv:0903.1219.
- [17] C. F. Berger et al., “Next-to-leading order QCD predictions for W+3-Jet distributions at hadron colliders”, *Phys. Rev. D* **80** (2009) 074036, doi:10.1103/PhysRevD.80.074036, arXiv:0907.1984.
- [18] C. F. Berger et al., “Precise Predictions for W+ 4-Jet Production at the Large Hadron Collider”, *Phys. Rev. Lett.* **106** (2011) 092001, doi:10.1103/PhysRevLett.106.092001, arXiv:1009.2338.
- [19] Z. Bern et al., “Ntuples for NLO events at hadron colliders”, *Comput. Phys. Commun.* **185** (2014) 1443, doi:10.1016/j.cpc.2014.01.011, arXiv:1310.7439.
- [20] CMS Collaboration, “The CMS experiment at the CERN LHC”, *JINST* **3** (2008) S08004, doi:10.1088/1748-0221/3/08/S08004.
- [21] CMS Collaboration, “Energy calibration and resolution of the CMS electromagnetic calorimeter in pp collisions at $\sqrt{s} = 7$ TeV”, *JINST* **8** (2013) P09009, doi:10.1088/1748-0221/8/09/P09009, arXiv:1306.2016.
- [22] GEANT4 Collaboration, “GEANT4—a simulation toolkit”, *Nucl. Instrum. Meth. A* **506** (2003) 250, doi:10.1016/S0168-9002(03)01368-8.
- [23] CMS Collaboration, “Charged particle multiplicities in pp interactions at $\sqrt{s} = 0.9, 2.36,$ and 7 TeV”, *JHEP* **01** (2010) 079, doi:10.1007/JHEP01(2011)079, arXiv:1011.5531.
- [24] P. Nason, “A new method for combining NLO QCD with shower Monte Carlo algorithms”, *JHEP* **11** (2004) 040, doi:10.1088/1126-6708/2004/11/040, arXiv:hep-ph/0409146.
- [25] S. Frixione, P. Nason, and C. Oleari, “Matching NLO QCD computations with parton shower simulations: the POWHEG method”, *JHEP* **11** (2007) 070, doi:10.1088/1126-6708/2007/11/070, arXiv:0709.2092.
- [26] S. Alioli, P. Nason, C. Oleari, and E. Re, “A general framework for implementing NLO calculations in shower Monte Carlo programs: the POWHEG BOX”, *JHEP* **06** (2010) 043, doi:10.1007/JHEP06(2010)043, arXiv:1002.2581.

- [27] S. Alioli, P. Nason, C. Oleari, and E. Re, “NLO single-top production matched with shower in POWHEG: s - and t -channel contributions”, *JHEP* **09** (2009) 111, doi:10.1088/1126-6708/2009/09/111, arXiv:0907.4076.
- [28] J. Pumplin et al., “New generation of parton distributions with uncertainties from global QCD analysis”, *JHEP* **07** (2002) 012, doi:10.1088/1126-6708/2002/07/012, arXiv:hep-ph/0201195.
- [29] K. Melnikov and F. Petriello, “Electroweak gauge boson production at hadron colliders through $O(\alpha_S^2)$ ”, *Phys. Rev. D* **74** (2006) 114017, doi:10.1103/PhysRevD.74.114017, arXiv:hep-ph/0609070.
- [30] J. Campbell, R. K. Ellis, and F. Tramontano, “Single top-quark production and decay at next-to-leading order”, *Phys. Rev. D* **70** (2004) 094012, doi:10.1103/PhysRevD.70.094012, arXiv:hep-ph/0408158.
- [31] J. Campbell and F. Tramontano, “Next-to-leading order corrections to Wt production and decay”, *Nucl. Phys. B* **726** (2005) 109, doi:10.1016/j.nuclphysb.2005.08.015, arXiv:hep-ph/0506289.
- [32] J. M. Campbell, R. Frederix, F. Maltoni, and F. Tramontano, “Next-to-Leading-Order Predictions for t -Channel Single-Top Production at Hadron Colliders”, *Phys. Rev. Lett.* **102** (2009) 182003, doi:10.1103/PhysRevLett.102.182003, arXiv:0903.0005.
- [33] J. M. Campbell, R. K. Ellis, and C. Williams, “Vector boson pair production at the LHC”, *JHEP* **07** (2011) 018, doi:10.1007/JHEP07(2011)018, arXiv:1105.0020.
- [34] M. Czakon, P. Fiedler, and A. Mitov, “The total top quark pair production cross-section at hadron colliders through $O(\alpha_S^4)$ ”, *Phys. Rev. Lett.* **110** (2013) 252004, doi:10.1103/PhysRevLett.110.252004, arXiv:1303.6254.
- [35] CMS Collaboration, “Performance of CMS muon reconstruction in pp collision events at $\sqrt{s} = 7$ TeV”, *JINST* **7** (2012) P10002, doi:10.1088/1748-0221/7/10/P10002, arXiv:1206.4071.
- [36] CMS Collaboration, “Particle-Flow Event Reconstruction in CMS and Performance for Jets, Taus, and E_T^{miss} ”, CMS Physics Analysis Summary CMS-PAS-PFT-09-001, 2009.
- [37] CMS Collaboration, “Commissioning of the Particle-flow Event Reconstruction with the first LHC collisions recorded in the CMS detector”, CMS Physics Analysis Summary CMS-PAS-PFT-10-001, 2010.
- [38] M. Cacciari, G. P. Salam, and G. Soyez, “The anti- k_t jet clustering algorithm”, *JHEP* **04** (2008) 063, doi:10.1088/1126-6708/2008/04/063, arXiv:0802.1189.
- [39] M. Cacciari, G. P. Salam, and G. Soyez, “FastJet user manual”, *Eur. Phys. J. C* **72** (2012) 1896, doi:10.1140/epjc/s10052-012-1896-2, arXiv:1111.6097.
- [40] CMS Collaboration, “Determination of jet energy calibration and transverse momentum resolution in CMS”, *JINST* **6** (2011) 11002, doi:10.1088/1748-0221/6/11/P11002, arXiv:1107.4277.
- [41] CMS Collaboration, “Measurement of the inclusive W and Z production cross sections in pp collisions at $\sqrt{s} = 7$ TeV with the CMS experiment”, *JHEP* **10** (2011) 132, doi:10.1007/JHEP10(2011)132, arXiv:1107.4789.

- [42] CMS Collaboration, “Identification of b-quark jets with the CMS experiment”, *JINST* **8** (2013) 04013, doi:10.1088/1748-0221/8/04/P04013, arXiv:1211.4462.
- [43] T. Adye, “Unfolding algorithms and tests using RooUnfold”, (2011).
arXiv:1105.1160.
- [44] CMS Collaboration, “Measurement of the inelastic proton-proton cross section at $\sqrt{s} = 7$ TeV”, *Phys. Lett. B* **722** (2013) 5, doi:10.1016/j.physletb.2013.03.024, arXiv:1210.6718.
- [45] H.-L. Lai et al., “New parton distributions for collider physics”, *Phys. Rev. D* **82** (2010) 074024, doi:10.1103/PhysRevD.82.074024, arXiv:1007.2241.
- [46] J. Gao et al., “CT10 next-to-next-to-leading order global analysis of QCD”, *Phys. Rev. D* **89** (2014) 033009, doi:10.1103/PhysRevD.89.033009, arXiv:1302.6246.
- [47] J. Alwall et al., “Comparative study of various algorithms for the merging of parton showers and matrix elements in hadronic collisions”, *Eur. Phys. J. C* **53** (2008) 473, doi:10.1140/epjc/s10052-007-0490-5, arXiv:0706.2569.
- [48] A. Buckley et al., “Rivet user manual”, *Comput. Phys. Commun.* **184** (2013) 2803, doi:10.1016/j.cpc.2013.05.021, arXiv:1003.0694.
- [49] Z. Bern et al., “Four-Jet Production at the Large Hadron Collider at Next-to-Leading Order in QCD”, *Phys. Rev. Lett.* **109** (2012) 042001, doi:10.1103/PhysRevLett.109.042001, arXiv:1112.3940.
- [50] A. D. Martin, W. J. Stirling, R. S. Thorne, and G. Watt, “Parton distributions for the LHC”, *Eur. Phys. J. C* **63** (2009) 189, doi:10.1140/epjc/s10052-009-1072-5, arXiv:0901.0002.
- [51] R. D. Ball et al., “A first unbiased global NLO determination of parton distributions and their uncertainties”, *Nucl. Phys. B* **838** (2010) 136, doi:10.1016/j.nuclphysb.2010.05.008, arXiv:1002.4407.
- [52] S. Alekhin et al., “The PDF4LHC Working Group Interim Report”, (2011).
arXiv:1101.0536.
- [53] M. Botje et al., “The PDF4LHC Working Group Interim Recommendations”, (2011).
arXiv:1101.0538.
- [54] D. Maître and S. Sapeta, “Simulated NNLO for high- p_T observables in vector boson + jets production at the LHC”, *Eur. Phys. J. C* **73** (2013) 2663, doi:10.1140/epjc/s10052-013-2663-8, arXiv:1307.2252.

A The CMS Collaboration

Yerevan Physics Institute, Yerevan, Armenia

V. Khachatryan, A.M. Sirunyan, A. Tumasyan

Institut für Hochenergiephysik der OeAW, Wien, Austria

W. Adam, T. Bergauer, M. Dragicevic, J. Erö, C. Fabjan¹, M. Friedl, R. Frühwirth¹, V.M. Ghete, C. Hartl, N. Hörmann, J. Hrubec, M. Jeitler¹, W. Kiesenhofer, V. Knünz, M. Krammer¹, I. Krätschmer, D. Liko, I. Mikulec, D. Rabady², B. Rahbaran, H. Rohringer, R. Schöfbeck, J. Strauss, A. Taurok, W. Treberer-Treberspurg, W. Waltenberger, C.-E. Wulz¹

National Centre for Particle and High Energy Physics, Minsk, Belarus

V. Mossolov, N. Shumeiko, J. Suarez Gonzalez

Universiteit Antwerpen, Antwerpen, Belgium

S. Alderweireldt, M. Bansal, S. Bansal, T. Cornelis, E.A. De Wolf, X. Janssen, A. Knutsson, S. Luyckx, S. Ochesanu, B. Roland, R. Rougny, M. Van De Klundert, H. Van Haevermaet, P. Van Mechelen, N. Van Remortel, A. Van Spilbeeck

Vrije Universiteit Brussel, Brussel, Belgium

F. Blekman, S. Blyweert, J. D'Hondt, N. Daci, N. Heracleous, A. Kalogeropoulos, J. Keaveney, T.J. Kim, S. Lowette, M. Maes, A. Olbrechts, Q. Python, D. Strom, S. Tavernier, W. Van Doninck, P. Van Mulders, G.P. Van Onsem, I. Vilella

Université Libre de Bruxelles, Bruxelles, Belgium

C. Caillol, B. Clerbaux, G. De Lentdecker, D. Dobur, L. Favart, A.P.R. Gay, A. Grebenyuk, A. Léonard, A. Mohammadi, L. Perniè², T. Reis, T. Seva, L. Thomas, C. Vander Velde, P. Vanlaer, J. Wang

Ghent University, Ghent, Belgium

V. Adler, K. Beernaert, L. Benucci, A. Cimmino, S. Costantini, S. Crucy, S. Dildick, A. Fagot, G. Garcia, B. Klein, J. Mccartin, A.A. Ocampo Rios, D. Ryckbosch, S. Salva Diblen, M. Sigamani, N. Strobbe, F. Thyssen, M. Tytgat, E. Yazgan, N. Zaganidis

Université Catholique de Louvain, Louvain-la-Neuve, Belgium

S. Basegmez, C. Beluffi³, G. Bruno, R. Castello, A. Caudron, L. Ceard, G.G. Da Silveira, C. Delaere, T. du Pree, D. Favart, L. Forthomme, A. Giammanco⁴, J. Hollar, P. Jez, M. Komm, V. Lemaître, J. Liao, C. Nuttens, D. Pagano, L. Perrini, A. Pin, K. Piotrkowski, A. Popov⁵, L. Quertenmont, M. Selvaggi, M. Vidal Marono, J.M. Vizan Garcia

Université de Mons, Mons, Belgium

N. Bely, T. Caebergs, E. Daubie, G.H. Hammad

Centro Brasileiro de Pesquisas Físicas, Rio de Janeiro, Brazil

W.L. Aldá Júnior, G.A. Alves, M. Correa Martins Junior, T. Dos Reis Martins, M.E. Pol

Universidade do Estado do Rio de Janeiro, Rio de Janeiro, Brazil

W. Carvalho, J. Chinellato⁶, A. Custódio, E.M. Da Costa, D. De Jesus Damiao, C. De Oliveira Martins, S. Fonseca De Souza, H. Malbouisson, M. Malek, D. Matos Figueiredo, L. Mundim, H. Nogima, W.L. Prado Da Silva, J. Santaolalla, A. Santoro, A. Sznajder, E.J. Tonelli Manganote⁶, A. Vilela Pereira

Universidade Estadual Paulista ^a, Universidade Federal do ABC ^b, São Paulo, Brazil

C.A. Bernardes^b, F.A. Dias^{a,7}, T.R. Fernandez Perez Tomei^a, E.M. Gregores^b, P.G. Mercadante^b, S.F. Novaes^a, Sandra S. Padula^a

Institute for Nuclear Research and Nuclear Energy, Sofia, Bulgaria

A. Aleksandrov, V. Genchev², P. Iaydjiev, A. Marinov, S. Piperov, M. Rodozov, G. Sultanov, M. Vutova

University of Sofia, Sofia, Bulgaria

A. Dimitrov, I. Glushkov, R. Hadjiiska, V. Kozhuharov, L. Litov, B. Pavlov, P. Petkov

Institute of High Energy Physics, Beijing, China

J.G. Bian, G.M. Chen, H.S. Chen, M. Chen, R. Du, C.H. Jiang, D. Liang, S. Liang, R. Plestina⁸, J. Tao, X. Wang, Z. Wang

State Key Laboratory of Nuclear Physics and Technology, Peking University, Beijing, China

C. Asawatangtrakuldee, Y. Ban, Y. Guo, Q. Li, W. Li, S. Liu, Y. Mao, S.J. Qian, D. Wang, L. Zhang, W. Zou

Universidad de Los Andes, Bogota, Colombia

C. Avila, L.F. Chaparro Sierra, C. Florez, J.P. Gomez, B. Gomez Moreno, J.C. Sanabria

Technical University of Split, Split, Croatia

N. Godinovic, D. Lelas, D. Polic, I. Puljak

University of Split, Split, Croatia

Z. Antunovic, M. Kovac

Institute Rudjer Boskovic, Zagreb, Croatia

V. Brigljevic, K. Kadija, J. Luetic, D. Mekterovic, L. Sudic

University of Cyprus, Nicosia, Cyprus

A. Attikis, G. Mavromanolakis, J. Mousa, C. Nicolaou, F. Ptochos, P.A. Razis

Charles University, Prague, Czech Republic

M. Bodlak, M. Finger, M. Finger Jr.⁹

Academy of Scientific Research and Technology of the Arab Republic of Egypt, Egyptian Network of High Energy Physics, Cairo, Egypt

Y. Assran¹⁰, A. Ellithi Kamel¹¹, M.A. Mahmoud¹², A. Radi^{13,14}

National Institute of Chemical Physics and Biophysics, Tallinn, Estonia

M. Kadastik, M. Murumaa, M. Raidal, A. Tiko

Department of Physics, University of Helsinki, Helsinki, Finland

P. Eerola, G. Fedi, M. Voutilainen

Helsinki Institute of Physics, Helsinki, Finland

J. Härkönen, V. Karimäki, R. Kinnunen, M.J. Kortelainen, T. Lampén, K. Lassila-Perini, S. Lehti, T. Lindén, P. Luukka, T. Mäenpää, T. Peltola, E. Tuominen, J. Tuominiemi, E. Tuovinen, L. Wendland

Lappeenranta University of Technology, Lappeenranta, Finland

T. Tuuva

DSM/IRFU, CEA/Saclay, Gif-sur-Yvette, France

M. Besancon, F. Couderc, M. Dejardin, D. Denegri, B. Fabbro, J.L. Faure, C. Favaro, F. Ferri, S. Ganjour, A. Givernaud, P. Gras, G. Hamel de Monchenault, P. Jarry, E. Locci, J. Malcles, J. Rander, A. Rosowsky, M. Titov

Laboratoire Leprince-Ringuet, Ecole Polytechnique, IN2P3-CNRS, Palaiseau, France

S. Baffioni, F. Beaudette, P. Busson, C. Charlot, T. Dahms, M. Dalchenko, L. Dobrzynski, N. Filipovic, A. Florent, R. Granier de Cassagnac, L. Mastrolorenzo, P. Miné, C. Mironov, I.N. Naranjo, M. Nguyen, C. Ochando, P. Paganini, R. Salerno, J.B. Sauvan, Y. Sirois, C. Veelken, Y. Yilmaz, A. Zabi

Institut Pluridisciplinaire Hubert Curien, Université de Strasbourg, Université de Haute Alsace Mulhouse, CNRS/IN2P3, Strasbourg, France

J.-L. Agram¹⁵, J. Andrea, A. Aubin, D. Bloch, J.-M. Brom, E.C. Chabert, C. Collard, E. Conte¹⁵, J.-C. Fontaine¹⁵, D. Gelé, U. Goerlach, C. Goetzmann, A.-C. Le Bihan, P. Van Hove

Centre de Calcul de l'Institut National de Physique Nucleaire et de Physique des Particules, CNRS/IN2P3, Villeurbanne, France

S. Gadrat

Université de Lyon, Université Claude Bernard Lyon 1, CNRS-IN2P3, Institut de Physique Nucléaire de Lyon, Villeurbanne, France

S. Beauceron, N. Beaupere, G. Boudoul², S. Brochet, C.A. Carrillo Montoya, J. Chasserat, R. Chierici, D. Contardo², P. Depasse, H. El Mamouni, J. Fan, J. Fay, S. Gascon, M. Gouzevitch, B. Ille, T. Kurca, M. Lethuillier, L. Mirabito, S. Perries, J.D. Ruiz Alvarez, D. Sabes, L. Sgandurra, V. Sordini, M. Vander Donckt, P. Verdier, S. Viret, H. Xiao

Institute of High Energy Physics and Informatization, Tbilisi State University, Tbilisi, Georgia

Z. Tsamalaidze⁹

RWTH Aachen University, I. Physikalisches Institut, Aachen, Germany

C. Autermann, S. Beranek, M. Bontenackels, M. Edelhoff, L. Feld, O. Hindrichs, K. Klein, A. Ostapchuk, A. Perieanu, F. Raupach, J. Sammet, S. Schael, D. Sprenger, H. Weber, B. Wittmer, V. Zhukov⁵

RWTH Aachen University, III. Physikalisches Institut A, Aachen, Germany

M. Ata, E. Dietz-Laursonn, D. Duchardt, M. Erdmann, R. Fischer, A. Güth, T. Hebbeker, C. Heidemann, K. Hoepfner, D. Klingebiel, S. Knutzen, P. Kreuzer, M. Merschmeyer, A. Meyer, M. Olschewski, K. Padeken, P. Papacz, H. Reithler, S.A. Schmitz, L. Sonnenschein, D. Teyssier, S. Thüer, M. Weber

RWTH Aachen University, III. Physikalisches Institut B, Aachen, Germany

V. Cherepanov, Y. Erdogan, G. Flügge, H. Geenen, M. Geisler, W. Haj Ahmad, F. Hoehle, B. Kargoll, T. Kress, Y. Kuessel, J. Lingemann², A. Nowack, I.M. Nugent, L. Perchalla, O. Pooth, A. Stahl

Deutsches Elektronen-Synchrotron, Hamburg, Germany

I. Asin, N. Bartosik, J. Behr, W. Behrenhoff, U. Behrens, A.J. Bell, M. Bergholz¹⁶, A. Bethani, K. Borras, A. Burgmeier, A. Cakir, L. Calligaris, A. Campbell, S. Choudhury, F. Costanza, C. Diez Pardos, S. Dooling, T. Dorland, G. Eckerlin, D. Eckstein, T. Eichhorn, G. Flucke, J. Garay Garcia, A. Geiser, P. Gunnellini, J. Hauk, G. Hellwig, M. Hempel, D. Horton, H. Jung, M. Kasemann, P. Katsas, J. Kieseler, C. Kleinwort, D. Krücker, W. Lange, J. Leonard, K. Lipka, A. Lobanov, W. Lohmann¹⁶, B. Lutz, R. Mankel, I. Marfin, I.-A. Melzer-Pellmann, A.B. Meyer, J. Mnich, A. Mussgiller, S. Naumann-Emme, A. Nayak, O. Novgorodova, F. Nowak, E. Ntomari, H. Perrey, D. Pitzl, R. Placakyte, A. Raspereza, P.M. Ribeiro Cipriano, E. Ron, M.Ö. Sahin, J. Salfeld-Nebgen, P. Saxena, R. Schmidt¹⁶, T. Schoerner-Sadenius, M. Schröder, S. Spannagel, A.D.R. Vargas Trevino, R. Walsh, C. Wissing

University of Hamburg, Hamburg, Germany

M. Aldaya Martin, V. Blobel, M. Centis Vignali, J. Erfle, E. Garutti, K. Goebel, M. Görner, M. Gosselink, J. Haller, M. Hoffmann, R.S. Höing, H. Kirschenmann, R. Klanner, R. Kogler, J. Lange, T. Lapsien, T. Lenz, I. Marchesini, J. Ott, T. Peiffer, N. Pietsch, D. Rathjens, C. Sander, H. Schettler, P. Schleper, E. Schlieckau, A. Schmidt, M. Seidel, J. Sibille¹⁷, V. Sola, H. Stadie, G. Steinbrück, D. Troendle, E. Usai, L. Vanelderen

Institut für Experimentelle Kernphysik, Karlsruhe, Germany

C. Barth, C. Baus, J. Berger, C. Böser, E. Butz, T. Chwalek, W. De Boer, A. Descroix, A. Dierlamm, M. Feindt, F. Frensch, M. Giffels, F. Hartmann², T. Hauth², U. Husemann, I. Katkov⁵, A. Kornmayer², E. Kuznetsova, P. Lobelle Pardo, M.U. Mozer, Th. Müller, A. Nürnberg, G. Quast, K. Rabbertz, F. Ratnikov, S. Röcker, H.J. Simonis, F.M. Stober, R. Ulrich, J. Wagner-Kuhr, S. Wayand, T. Weiler, R. Wolf

Institute of Nuclear and Particle Physics (INPP), NCSR Demokritos, Aghia Paraskevi, Greece

G. Anagnostou, G. Daskalakis, T. Gerasis, V.A. Giakoumopoulou, A. Kyriakis, D. Loukas, A. Markou, C. Markou, A. Psallidas, I. Topsis-Giotis

University of Athens, Athens, Greece

A. Panagiotou, N. Saoulidou, E. Stiliaris

University of Ioánnina, Ioánnina, Greece

X. Aslanoglou, I. Evangelou, G. Flouris, C. Foudas, P. Kokkas, N. Manthos, I. Papadopoulos, E. Paradas

Wigner Research Centre for Physics, Budapest, Hungary

G. Bencze, C. Hajdu, P. Hidas, D. Horvath¹⁸, F. Sikler, V. Veszpremi, G. Vesztergombi¹⁹, A.J. Zsigmond

Institute of Nuclear Research ATOMKI, Debrecen, Hungary

N. Beni, S. Czellar, J. Karancsi²⁰, J. Molnar, J. Palinkas, Z. Szillasi

University of Debrecen, Debrecen, Hungary

P. Raics, Z.L. Trocsanyi, B. Ujvari

National Institute of Science Education and Research, Bhubaneswar, India

S.K. Swain

Panjab University, Chandigarh, India

S.B. Beri, V. Bhatnagar, N. Dhingra, R. Gupta, A.K. Kalsi, M. Kaur, M. Mittal, N. Nishu, J.B. Singh

University of Delhi, Delhi, India

Ashok Kumar, Arun Kumar, S. Ahuja, A. Bhardwaj, B.C. Choudhary, A. Kumar, S. Malhotra, M. Naimuddin, K. Ranjan, V. Sharma

Saha Institute of Nuclear Physics, Kolkata, India

S. Banerjee, S. Bhattacharya, K. Chatterjee, S. Dutta, B. Gomber, Sa. Jain, Sh. Jain, R. Khurana, A. Modak, S. Mukherjee, D. Roy, S. Sarkar, M. Sharan

Bhabha Atomic Research Centre, Mumbai, India

A. Abdulsalam, D. Dutta, S. Kailas, V. Kumar, A.K. Mohanty², L.M. Pant, P. Shukla, A. Topkar

Tata Institute of Fundamental Research, Mumbai, India

T. Aziz, S. Banerjee, R.M. Chatterjee, R.K. Dewanjee, S. Dugad, S. Ganguly, S. Ghosh,

M. Guchait, A. Gurtu²¹, G. Kole, S. Kumar, M. Maity²², G. Majumder, K. Mazumdar, G.B. Mohanty, B. Parida, K. Sudhakar, N. Wickramage²³

Institute for Research in Fundamental Sciences (IPM), Tehran, Iran

H. Bakhshiansohi, H. Behnamian, S.M. Etesami²⁴, A. Fahim²⁵, R. Goldouzian, A. Jafari, M. Khakzad, M. Mohammadi Najafabadi, M. Naseri, S. Paktinat Mehdiabadi, B. Safarzadeh²⁶, M. Zeinali

University College Dublin, Dublin, Ireland

M. Felcini, M. Grunewald

INFN Sezione di Bari ^a, Università di Bari ^b, Politecnico di Bari ^c, Bari, Italy

M. Abbrescia^{a,b}, L. Barbone^{a,b}, C. Calabria^{a,b}, S.S. Chhibra^{a,b}, A. Colaleo^a, D. Creanza^{a,c}, N. De Filippis^{a,c}, M. De Palma^{a,b}, L. Fiore^a, G. Iaselli^{a,c}, G. Maggi^{a,c}, M. Maggi^a, S. My^{a,c}, S. Nuzzo^{a,b}, A. Pompili^{a,b}, G. Pugliese^{a,c}, R. Radogna^{a,b,2}, G. Selvaggi^{a,b}, L. Silvestris^{a,2}, G. Singh^{a,b}, R. Venditti^{a,b}, P. Verwilligen^a, G. Zito^a

INFN Sezione di Bologna ^a, Università di Bologna ^b, Bologna, Italy

G. Abbiendi^a, A.C. Benvenuti^a, D. Bonacorsi^{a,b}, S. Braibant-Giacomelli^{a,b}, L. Brigliadori^{a,b}, R. Campanini^{a,b}, P. Capiluppi^{a,b}, A. Castro^{a,b}, F.R. Cavallo^a, G. Codispoti^{a,b}, M. Cuffiani^{a,b}, G.M. Dallavalle^a, F. Fabbri^a, A. Fanfani^{a,b}, D. Fasanella^{a,b}, P. Giacomelli^a, C. Grandi^a, L. Guiducci^{a,b}, S. Marcellini^a, G. Masetti^{a,2}, A. Montanari^a, F.L. Navarria^{a,b}, A. Perrotta^a, F. Primavera^{a,b}, A.M. Rossi^{a,b}, T. Rovelli^{a,b}, G.P. Siroli^{a,b}, N. Tosi^{a,b}, R. Travaglini^{a,b}

INFN Sezione di Catania ^a, Università di Catania ^b, CSFNSM ^c, Catania, Italy

S. Albergo^{a,b}, G. Cappello^a, M. Chiorboli^{a,b}, S. Costa^{a,b}, F. Giordano^{a,2}, R. Potenza^{a,b}, A. Tricomi^{a,b}, C. Tuve^{a,b}

INFN Sezione di Firenze ^a, Università di Firenze ^b, Firenze, Italy

G. Barbagli^a, V. Ciulli^{a,b}, C. Civinini^a, R. D'Alessandro^{a,b}, E. Focardi^{a,b}, E. Gallo^a, S. Gonzi^{a,b}, V. Gori^{a,b,2}, P. Lenzi^{a,b}, M. Meschini^a, S. Paoletti^a, G. Sguazzoni^a, A. Tropiano^{a,b}

INFN Laboratori Nazionali di Frascati, Frascati, Italy

L. Benussi, S. Bianco, F. Fabbri, D. Piccolo

INFN Sezione di Genova ^a, Università di Genova ^b, Genova, Italy

F. Ferro^a, M. Lo Vetere^{a,b}, E. Robutti^a, S. Tosi^{a,b}

INFN Sezione di Milano-Bicocca ^a, Università di Milano-Bicocca ^b, Milano, Italy

M.E. Dinardo^{a,b}, S. Fiorendi^{a,b,2}, S. Gennai^{a,2}, R. Gerosa², A. Ghezzi^{a,b}, P. Govoni^{a,b}, M.T. Lucchini^{a,b,2}, S. Malvezzi^a, R.A. Manzoni^{a,b}, A. Martelli^{a,b}, B. Marzocchi, D. Menasce^a, L. Moroni^a, M. Paganoni^{a,b}, D. Pedrini^a, S. Ragazzi^{a,b}, N. Redaelli^a, T. Tabarelli de Fatis^{a,b}

INFN Sezione di Napoli ^a, Università di Napoli 'Federico II' ^b, Università della Basilicata (Potenza) ^c, Università G. Marconi (Roma) ^d, Napoli, Italy

S. Buontempo^a, N. Cavallo^{a,c}, S. Di Guida^{a,d,2}, F. Fabozzi^{a,c}, A.O.M. Iorio^{a,b}, L. Lista^a, S. Meola^{a,d,2}, M. Merola^a, P. Paolucci^{a,2}

INFN Sezione di Padova ^a, Università di Padova ^b, Università di Trento (Trento) ^c, Padova, Italy

P. Azzi^a, N. Bacchetta^a, M. Bellato^a, D. Bisello^{a,b}, A. Branca^{a,b}, R. Carlin^{a,b}, P. Checchia^a, M. Dall'Osso^{a,b}, T. Dorigo^a, M. Galanti^{a,b}, F. Gasparini^{a,b}, U. Gasparini^{a,b}, P. Giubilato^{a,b}, A. Gozzelino^a, K. Kanishchev^{a,c}, S. Lacaprara^a, M. Margoni^{a,b}, A.T. Meneguzzo^{a,b}, J. Pazzini^{a,b}, N. Pozzobon^{a,b}, P. Ronchese^{a,b}, M. Sgaravatto^a, M. Tosi^{a,b}, A. Triossi^a, S. Ventura^a, A. Zucchetta^{a,b}, G. Zumerle^{a,b}

INFN Sezione di Pavia ^a, Università di Pavia ^b, Pavia, ItalyS.P. Ratti^{a,b}, C. Riccardi^{a,b}, P. Salvini^a, P. Vitulo^{a,b}**INFN Sezione di Perugia ^a, Università di Perugia ^b, Perugia, Italy**M. Biasini^{a,b}, G.M. Bilei^a, D. Ciangottini^{a,b}, L. Fanò^{a,b}, P. Lariccia^{a,b}, G. Mantovani^{a,b}, M. Menichelli^a, F. Romeo^{a,b}, A. Saha^a, A. Santocchia^{a,b}, A. Spiezia^{a,b,2}**INFN Sezione di Pisa ^a, Università di Pisa ^b, Scuola Normale Superiore di Pisa ^c, Pisa, Italy**K. Androsov^{a,27}, P. Azzurri^a, G. Bagliesi^a, J. Bernardini^a, T. Boccali^a, G. Broccolo^{a,c}, R. Castaldi^a, M.A. Ciocci^{a,27}, R. Dell'Orso^a, S. Donato^{a,c}, F. Fiori^{a,c}, L. Foà^{a,c}, A. Giassi^a, M.T. Grippo^{a,27}, F. Ligabue^{a,c}, T. Lomtadze^a, L. Martini^{a,b}, A. Messineo^{a,b}, C.S. Moon^{a,28}, F. Palla^{a,2}, A. Rizzi^{a,b}, A. Savoy-Navarro^{a,29}, A.T. Serban^a, P. Spagnolo^a, P. Squillacioti^{a,27}, R. Tenchini^a, G. Tonelli^{a,b}, A. Venturi^a, P.G. Verdini^a, C. Vernieri^{a,c,2}**INFN Sezione di Roma ^a, Università di Roma ^b, Roma, Italy**L. Barone^{a,b}, F. Cavallari^a, D. Del Re^{a,b}, M. Diemoz^a, M. Grassi^{a,b}, C. Jorda^a, E. Longo^{a,b}, F. Margaroli^{a,b}, P. Meridiani^a, F. Micheli^{a,b,2}, S. Nourbakhsh^{a,b}, G. Organtini^{a,b}, R. Paramatti^a, S. Rahatlou^{a,b}, C. Rovelli^a, F. Santanastasio^{a,b}, L. Soffi^{a,b,2}, P. Traczyk^{a,b}**INFN Sezione di Torino ^a, Università di Torino ^b, Università del Piemonte Orientale (Novara) ^c, Torino, Italy**N. Amapane^{a,b}, R. Arcidiacono^{a,c}, S. Argiro^{a,b,2}, M. Arneodo^{a,c}, R. Bellan^{a,b}, C. Biino^a, N. Cartiglia^a, S. Casasso^{a,b,2}, M. Costa^{a,b}, A. Degano^{a,b}, N. Demaria^a, L. Finco^{a,b}, C. Mariotti^a, S. Maselli^a, E. Migliore^{a,b}, V. Monaco^{a,b}, M. Musich^a, M.M. Obertino^{a,c,2}, G. Ortona^{a,b}, L. Pacher^{a,b}, N. Pastrone^a, M. Pelliccioni^a, G.L. Pinna Angioni^{a,b}, A. Potenza^{a,b}, A. Romero^{a,b}, M. Ruspa^{a,c}, R. Sacchi^{a,b}, A. Solano^{a,b}, A. Staiano^a, U. Tamponi^a**INFN Sezione di Trieste ^a, Università di Trieste ^b, Trieste, Italy**S. Belforte^a, V. Candelise^{a,b}, M. Casarsa^a, F. Cossutti^a, G. Della Ricca^{a,b}, B. Gobbo^a, C. La Licata^{a,b}, M. Marone^{a,b}, D. Montanino^{a,b}, A. Schizzi^{a,b,2}, T. Umer^{a,b}, A. Zanetti^a**Kangwon National University, Chunchon, Korea**

S. Chang, A. Kropivnitskaya, S.K. Nam

Kyungpook National University, Daegu, Korea

D.H. Kim, G.N. Kim, M.S. Kim, D.J. Kong, S. Lee, Y.D. Oh, H. Park, A. Sakharov, D.C. Son

Chonnam National University, Institute for Universe and Elementary Particles, Kwangju, Korea

J.Y. Kim, S. Song

Korea University, Seoul, Korea

S. Choi, D. Gyun, B. Hong, M. Jo, H. Kim, Y. Kim, B. Lee, K.S. Lee, S.K. Park, Y. Roh

University of Seoul, Seoul, Korea

M. Choi, H. Kim, J.H. Kim, I.C. Park, S. Park, G. Ryu, M.S. Ryu

Sungkyunkwan University, Suwon, Korea

Y. Choi, Y.K. Choi, J. Goh, E. Kwon, J. Lee, H. Seo, I. Yu

Vilnius University, Vilnius, Lithuania

A. Juodagalvis

National Centre for Particle Physics, Universiti Malaya, Kuala Lumpur, Malaysia

J.R. Komaragiri

Centro de Investigacion y de Estudios Avanzados del IPN, Mexico City, Mexico

H. Castilla-Valdez, E. De La Cruz-Burelo, I. Heredia-de La Cruz³⁰, R. Lopez-Fernandez, A. Sanchez-Hernandez

Universidad Iberoamericana, Mexico City, Mexico

S. Carrillo Moreno, F. Vazquez Valencia

Benemerita Universidad Autonoma de Puebla, Puebla, Mexico

I. Pedraza, H.A. Salazar Ibarguen

Universidad Autónoma de San Luis Potosí, San Luis Potosí, Mexico

E. Casimiro Linares, A. Morelos Pineda

University of Auckland, Auckland, New Zealand

D. Krofcheck

University of Canterbury, Christchurch, New Zealand

P.H. Butler, S. Reucroft

National Centre for Physics, Quaid-I-Azam University, Islamabad, Pakistan

A. Ahmad, M. Ahmad, Q. Hassan, H.R. Hoorani, S. Khalid, W.A. Khan, T. Khurshid, M.A. Shah, M. Shoaib

National Centre for Nuclear Research, Swierk, Poland

H. Bialkowska, M. Bluj, B. Boimska, T. Frueboes, M. Górski, M. Kazana, K. Nawrocki, K. Romanowska-Rybinska, M. Szleper, P. Zalewski

Institute of Experimental Physics, Faculty of Physics, University of Warsaw, Warsaw, Poland

G. Brona, K. Bunkowski, M. Cwiok, W. Dominik, K. Doroba, A. Kalinowski, M. Konecki, J. Krolikowski, M. Misiura, M. Olszewski, W. Wolszczak

Laboratório de Instrumentação e Física Experimental de Partículas, Lisboa, Portugal

P. Bargassa, C. Beirão Da Cruz E Silva, P. Faccioli, P.G. Ferreira Parracho, M. Gallinaro, F. Nguyen, J. Rodrigues Antunes, J. Seixas, J. Varela, P. Vischia

Joint Institute for Nuclear Research, Dubna, Russia

I. Golutvin, V. Karjavin, V. Konoplyanikov, V. Korenkov, G. Kozlov, A. Lanev, A. Malakhov, V. Matveev³¹, V.V. Mitsyn, P. Moisenz, V. Palichik, V. Perelygin, S. Shmatov, S. Shulha, N. Skatchkov, V. Smirnov, E. Tikhonenko, A. Zarubin

Petersburg Nuclear Physics Institute, Gatchina (St. Petersburg), Russia

V. Golovtsov, Y. Ivanov, V. Kim³², P. Levchenko, V. Murzin, V. Oreshkin, I. Smirnov, V. Sulimov, L. Uvarov, S. Vavilov, A. Vorobyev, An. Vorobyev

Institute for Nuclear Research, Moscow, Russia

Yu. Andreev, A. Dermenev, S. Gninenko, N. Golubev, M. Kirsanov, N. Krasnikov, A. Pashenkov, D. Tlisov, A. Toropin

Institute for Theoretical and Experimental Physics, Moscow, Russia

V. Epshteyn, V. Gavrilov, N. Lychkovskaya, V. Popov, G. Safronov, S. Semenov, A. Spiridonov, V. Stolin, E. Vlasov, A. Zhokin

P.N. Lebedev Physical Institute, Moscow, Russia

V. Andreev, M. Azarkin, I. Dremin, M. Kirakosyan, A. Leonidov, G. Mesyats, S.V. Rusakov, A. Vinogradov

Skobeltsyn Institute of Nuclear Physics, Lomonosov Moscow State University, Moscow, Russia

A. Belyaev, E. Boos, M. Dubinin⁷, L. Dudko, A. Ershov, A. Gribushin, V. Klyukhin, O. Kodolova, I. Lokhtin, S. Obraztsov, S. Petrushanko, V. Savrin, A. Snigirev

State Research Center of Russian Federation, Institute for High Energy Physics, Protvino, Russia

I. Azhgirey, I. Bayshev, S. Bitioukov, V. Kachanov, A. Kalinin, D. Konstantinov, V. Krychkin, V. Petrov, R. Ryutin, A. Sobol, L. Tourtchanovitch, S. Troshin, N. Tyurin, A. Uzunian, A. Volkov

University of Belgrade, Faculty of Physics and Vinca Institute of Nuclear Sciences, Belgrade, Serbia

P. Adzic³³, M. Dordevic, M. Ekmedzic, J. Milosevic

Centro de Investigaciones Energéticas Medioambientales y Tecnológicas (CIEMAT), Madrid, Spain

J. Alcaraz Maestre, C. Battilana, E. Calvo, M. Cerrada, M. Chamizo Llatas², N. Colino, B. De La Cruz, A. Delgado Peris, D. Domínguez Vázquez, A. Escalante Del Valle, C. Fernandez Bedoya, J.P. Fernández Ramos, J. Flix, M.C. Fouz, P. Garcia-Abia, O. Gonzalez Lopez, S. Goy Lopez, J.M. Hernandez, M.I. Josa, G. Merino, E. Navarro De Martino, A. Pérez-Calero Yzquierdo, J. Puerta Pelayo, A. Quintario Olmeda, I. Redondo, L. Romero, M.S. Soares

Universidad Autónoma de Madrid, Madrid, Spain

C. Albajar, J.F. de Trocóniz, M. Missiroli

Universidad de Oviedo, Oviedo, Spain

H. Brun, J. Cuevas, J. Fernandez Menendez, S. Folgueras, I. Gonzalez Caballero, L. Lloret Iglesias

Instituto de Física de Cantabria (IFCA), CSIC-Universidad de Cantabria, Santander, Spain

J.A. Brochero Cifuentes, I.J. Cabrillo, A. Calderon, J. Duarte Campderros, M. Fernandez, G. Gomez, A. Graziano, A. Lopez Virto, J. Marco, R. Marco, C. Martinez Rivero, F. Matorras, F.J. Munoz Sanchez, J. Piedra Gomez, T. Rodrigo, A.Y. Rodríguez-Marrero, A. Ruiz-Jimeno, L. Scodellaro, I. Vila, R. Vilar Cortabitarte

CERN, European Organization for Nuclear Research, Geneva, Switzerland

D. Abbaneo, E. Auffray, G. Auzinger, M. Bachtis, P. Baillon, A.H. Ball, D. Barney, A. Benaglia, J. Bendavid, L. Benhabib, J.F. Benitez, C. Bernet⁸, G. Bianchi, P. Bloch, A. Bocci, A. Bonato, O. Bondu, C. Botta, H. Breuker, T. Camporesi, G. Cerminara, S. Colafranceschi³⁴, M. D'Alfonso, D. d'Enterria, A. Dabrowski, A. David, F. De Guio, A. De Roeck, S. De Visscher, M. Dobson, N. Dupont-Sagorin, A. Elliott-Peisert, J. Eugster, G. Franzoni, W. Funk, D. Gigi, K. Gill, D. Giordano, M. Girone, F. Glege, R. Guida, S. Gundacker, M. Guthoff, J. Hammer, M. Hansen, P. Harris, J. Hegeman, V. Innocente, P. Janot, K. Kousouris, K. Krajczar, P. Lecoq, C. Lourenço, N. Magini, L. Malgeri, M. Mannelli, J. Marrouche, L. Masetti, F. Meijers, S. Mersi, E. Meschi, F. Moortgat, S. Morovic, M. Mulders, P. Musella, L. Orsini, L. Pape, E. Perez, L. Perrozzi, A. Petrilli, G. Petrucciani, A. Pfeiffer, M. Pierini, M. Pimiä, D. Piparo, M. Plagge, A. Racz, G. Rolandi³⁵, M. Rovere, H. Sakulin, C. Schäfer, C. Schwick, S. Sekmen, A. Sharma, P. Siegrist, P. Silva, M. Simon, P. Sphicas³⁶, D. Spiga, J. Steggemann, B. Stieger, M. Stoye, D. Treille, A. Tsiros, G.I. Veres¹⁹, J.R. Vlimant, N. Wardle, H.K. Wöhri, W.D. Zeuner

Paul Scherrer Institut, Villigen, Switzerland

W. Bertl, K. Deiters, W. Erdmann, R. Horisberger, Q. Ingram, H.C. Kaestli, S. König, D. Kotlinski, U. Langenegger, D. Renker, T. Rohe

Institute for Particle Physics, ETH Zurich, Zurich, Switzerland

F. Bachmair, L. Bäni, L. Bianchini, P. Bortignon, M.A. Buchmann, B. Casal, N. Chanon, A. Deisher, G. Dissertori, M. Dittmar, M. Donegà, M. Dünser, P. Eller, C. Grab, D. Hits, W. Lustermann, B. Mangano, A.C. Marini, P. Martinez Ruiz del Arbol, D. Meister, N. Mohr, C. Nägeli³⁷, P. Nef, F. Nessi-Tedaldi, F. Pandolfi, F. Pauss, M. Peruzzi, M. Quittnat, L. Rebane, F.J. Ronga, M. Rossini, A. Starodumov³⁸, M. Takahashi, K. Theofilatos, R. Wallny, H.A. Weber

Universität Zürich, Zurich, Switzerland

C. Amsler³⁹, M.F. Canelli, V. Chiochia, A. De Cosa, A. Hinzmann, T. Hreus, M. Ivova Rikova, B. Kilminster, B. Millan Mejias, J. Ngadiuba, P. Robmann, H. Snoek, S. Taroni, M. Verzetti, Y. Yang

National Central University, Chung-Li, Taiwan

M. Cardaci, K.H. Chen, C. Ferro, C.M. Kuo, W. Lin, Y.J. Lu, R. Volpe, S.S. Yu

National Taiwan University (NTU), Taipei, Taiwan

P. Chang, Y.H. Chang, Y.W. Chang, Y. Chao, K.F. Chen, P.H. Chen, C. Dietz, U. Grundler, W.-S. Hou, K.Y. Kao, Y.J. Lei, Y.F. Liu, R.-S. Lu, D. Majumder, E. Petrakou, Y.M. Tzeng, R. Wilken

Chulalongkorn University, Faculty of Science, Department of Physics, Bangkok, Thailand

B. Asavapibhop, N. Srimanobhas, N. Suwonjandee

Cukurova University, Adana, Turkey

A. Adiguzel, M.N. Bakirci⁴⁰, S. Cerci⁴¹, C. Dozen, I. Dumanoglu, E. Eskut, S. Girgis, G. Gokbulut, E. Gurpinar, I. Hos, E.E. Kangal, A. Kayis Topaksu, G. Onengut⁴², K. Ozdemir, S. Ozturk⁴⁰, A. Polatoz, K. Sogut⁴³, D. Sunar Cerci⁴¹, B. Tali⁴¹, H. Topakli⁴⁰, M. Vergili

Middle East Technical University, Physics Department, Ankara, Turkey

I.V. Akin, B. Bilin, S. Bilmis, H. Gamsizkan, G. Karapinar⁴⁴, K. Ocalan, U.E. Surat, M. Yalvac, M. Zeyrek

Bogazici University, Istanbul, Turkey

E. Gülmez, B. Isildak⁴⁵, M. Kaya⁴⁶, O. Kaya⁴⁶

Istanbul Technical University, Istanbul, Turkey

H. Bahtiyar⁴⁷, E. Barlas, K. Cankocak, F.I. Vardarli, M. Yücel

National Scientific Center, Kharkov Institute of Physics and Technology, Kharkov, Ukraine

L. Levchuk, P. Sorokin

University of Bristol, Bristol, United Kingdom

J.J. Brooke, E. Clement, D. Cussans, H. Flacher, R. Frazier, J. Goldstein, M. Grimes, G.P. Heath, H.F. Heath, J. Jacob, L. Kreczko, C. Lucas, Z. Meng, D.M. Newbold⁴⁸, S. Paramesvaran, A. Poll, S. Senkin, V.J. Smith, T. Williams

Rutherford Appleton Laboratory, Didcot, United Kingdom

K.W. Bell, A. Belyaev⁴⁹, C. Brew, R.M. Brown, D.J.A. Cockerill, J.A. Coughlan, K. Harder, S. Harper, E. Olaiya, D. Petyt, C.H. Shepherd-Themistocleous, A. Thea, I.R. Tomalin, W.J. Womersley, S.D. Worm

Imperial College, London, United Kingdom

M. Baber, R. Bainbridge, O. Buchmuller, D. Burton, D. Colling, N. Cripps, M. Cutajar, P. Dauncey, G. Davies, M. Della Negra, P. Dunne, W. Ferguson, J. Fulcher, D. Futyan, A. Gilbert, G. Hall, G. Iles, M. Jarvis, G. Karapostoli, M. Kenzie, R. Lane, R. Lucas⁴⁸, L. Lyons, A.-M. Magnan, S. Malik, B. Mathias, J. Nash, A. Nikitenko³⁸, J. Pela, M. Pesaresi, K. Petridis,

D.M. Raymond, S. Rogerson, A. Rose, C. Seez, P. Sharp[†], A. Tapper, M. Vazquez Acosta, T. Virdee

Brunel University, Uxbridge, United Kingdom

J.E. Cole, P.R. Hobson, A. Khan, P. Kyberd, D. Leggat, D. Leslie, W. Martin, I.D. Reid, P. Symonds, L. Teodorescu, M. Turner

Baylor University, Waco, USA

J. Dittmann, K. Hatakeyama, A. Kasmi, H. Liu, T. Scarborough

The University of Alabama, Tuscaloosa, USA

O. Charaf, S.I. Cooper, C. Henderson, P. Rumerio

Boston University, Boston, USA

A. Avetisyan, T. Bose, C. Fantasia, A. Heister, P. Lawson, C. Richardson, J. Rohlf, D. Sperka, J. St. John, L. Sulak

Brown University, Providence, USA

J. Alimena, S. Bhattacharya, G. Christopher, D. Cutts, Z. Demiragli, A. Ferapontov, A. Garabedian, U. Heintz, S. Jabeen, G. Kukartsev, E. Laird, G. Landsberg, M. Luk, M. Narain, M. Segala, T. Sinthuprasith, T. Speer, J. Swanson

University of California, Davis, Davis, USA

R. Breedon, G. Breto, M. Calderon De La Barca Sanchez, S. Chauhan, M. Chertok, J. Conway, R. Conway, P.T. Cox, R. Erbacher, M. Gardner, W. Ko, R. Lander, T. Miceli, M. Mulhearn, D. Pellett, J. Pilot, F. Ricci-Tam, M. Searle, S. Shalhout, J. Smith, M. Squires, D. Stolp, M. Tripathi, S. Wilbur, R. Yohay

University of California, Los Angeles, USA

R. Cousins, P. Everaerts, C. Farrell, J. Hauser, M. Ignatenko, G. Rakness, E. Takasugi, V. Valuev, M. Weber

University of California, Riverside, Riverside, USA

J. Babb, R. Clare, J. Ellison, J.W. Gary, G. Hanson, J. Heilman, P. Jandir, E. Kennedy, F. Lacroix, H. Liu, O.R. Long, A. Luthra, M. Malberti, H. Nguyen, A. Shrinivas, S. Sumowidagdo, S. Wimpenny

University of California, San Diego, La Jolla, USA

W. Andrews, J.G. Branson, G.B. Cerati, S. Cittolin, R.T. D'Agnolo, D. Evans, A. Holzner, R. Kelley, D. Klein, M. Lebourgeois, J. Letts, I. Macneill, D. Olivito, S. Padhi, C. Palmer, M. Pieri, M. Sani, V. Sharma, S. Simon, E. Sudano, M. Tadel, Y. Tu, A. Vartak, C. Welke, F. Würthwein, A. Yagil, J. Yoo

University of California, Santa Barbara, Santa Barbara, USA

D. Barge, J. Bradmiller-Feld, C. Campagnari, T. Danielson, A. Dishaw, K. Flowers, M. Franco Sevilla, P. Geffert, C. George, F. Golf, L. Gouskos, J. Incandela, C. Justus, N. Mccoll, J. Richman, D. Stuart, W. To, C. West

California Institute of Technology, Pasadena, USA

A. Apresyan, A. Bornheim, J. Bunn, Y. Chen, E. Di Marco, J. Duarte, A. Mott, H.B. Newman, C. Pena, C. Rogan, M. Spiropulu, V. Timciuc, R. Wilkinson, S. Xie, R.Y. Zhu

Carnegie Mellon University, Pittsburgh, USA

V. Azzolini, A. Calamba, T. Ferguson, Y. Iiyama, M. Paulini, J. Russ, H. Vogel, I. Vorobiev

University of Colorado at Boulder, Boulder, USA

J.P. Cumalat, B.R. Drell, W.T. Ford, A. Gaz, E. Luiggi Lopez, U. Nauenberg, J.G. Smith, K. Stenson, K.A. Ulmer, S.R. Wagner

Cornell University, Ithaca, USA

J. Alexander, A. Chatterjee, J. Chu, S. Dittmer, N. Eggert, W. Hopkins, N. Mirman, G. Nicolas Kaufman, J.R. Patterson, A. Ryd, E. Salvati, L. Skinnari, W. Sun, W.D. Teo, J. Thom, J. Thompson, J. Tucker, Y. Weng, L. Winstrom, P. Wittich

Fairfield University, Fairfield, USA

D. Winn

Fermi National Accelerator Laboratory, Batavia, USA

S. Abdullin, M. Albrow, J. Anderson, G. Apollinari, L.A.T. Bauerdick, A. Beretvas, J. Berryhill, P.C. Bhat, K. Burkett, J.N. Butler, H.W.K. Cheung, F. Chlebana, S. Cihangir, V.D. Elvira, I. Fisk, J. Freeman, Y. Gao, E. Gottschalk, L. Gray, D. Green, S. Grünendahl, O. Gutsche, J. Hanlon, D. Hare, R.M. Harris, J. Hirschauer, B. Hooberman, S. Jindariani, M. Johnson, U. Joshi, K. Kaadze, B. Klima, B. Kreis, S. Kwan, J. Linacre, D. Lincoln, R. Lipton, T. Liu, J. Lykken, K. Maeshima, J.M. Marraffino, V.I. Martinez Outschoorn, S. Maruyama, D. Mason, P. McBride, K. Mishra, S. Mrenna, Y. Musienko³¹, S. Nahn, C. Newman-Holmes, V. O'Dell, O. Prokofyev, E. Sexton-Kennedy, S. Sharma, A. Soha, W.J. Spalding, L. Spiegel, L. Taylor, S. Tkaczyk, N.V. Tran, L. Uplegger, E.W. Vaandering, R. Vidal, A. Whitbeck, J. Whitmore, F. Yang

University of Florida, Gainesville, USA

D. Acosta, P. Avery, D. Bourilkov, M. Carver, T. Cheng, D. Curry, S. Das, M. De Gruttola, G.P. Di Giovanni, R.D. Field, M. Fisher, I.K. Furic, J. Hugon, J. Konigsberg, A. Korytov, T. Kypreos, J.F. Low, K. Matchev, P. Milenovic⁵⁰, G. Mitselmakher, L. Muniz, A. Rinkevicius, L. Shchutska, N. Skhirtladze, M. Snowball, J. Yelton, M. Zakaria

Florida International University, Miami, USA

V. Gaultney, S. Hewamanage, S. Linn, P. Markowitz, G. Martinez, J.L. Rodriguez

Florida State University, Tallahassee, USA

T. Adams, A. Askew, J. Bochenek, B. Diamond, J. Haas, S. Hagopian, V. Hagopian, K.F. Johnson, H. Prosper, V. Veeraraghavan, M. Weinberg

Florida Institute of Technology, Melbourne, USA

M.M. Baarmand, M. Hohlmann, H. Kalakhety, F. Yumiceva

University of Illinois at Chicago (UIC), Chicago, USA

M.R. Adams, L. Apanasevich, V.E. Bazterra, D. Berry, R.R. Betts, I. Bucinskaite, R. Cavanaugh, O. Evdokimov, L. Gauthier, C.E. Gerber, D.J. Hofman, S. Khalatyan, P. Kurt, D.H. Moon, C. O'Brien, C. Silkworth, P. Turner, N. Varelas

The University of Iowa, Iowa City, USA

E.A. Albayrak⁴⁷, B. Bilki⁵¹, W. Clarida, K. Dilsiz, F. Duru, M. Haytmyradov, J.-P. Merlo, H. Mermerkaya⁵², A. Mestvirishvili, A. Moeller, J. Nachtman, H. Ogul, Y. Onel, F. Ozok⁴⁷, A. Penzo, R. Rahmat, S. Sen, P. Tan, E. Tiras, J. Wetzel, T. Yetkin⁵³, K. Yi

Johns Hopkins University, Baltimore, USA

B.A. Barnett, B. Blumenfeld, S. Bolognesi, D. Fehling, A.V. Gritsan, P. Maksimovic, C. Martin, M. Swartz

The University of Kansas, Lawrence, USA

P. Baringer, A. Bean, G. Benelli, C. Bruner, J. Gray, R.P. Kenny III, M. Murray, D. Noonan, S. Sanders, J. Sekaric, R. Stringer, Q. Wang, J.S. Wood

Kansas State University, Manhattan, USA

A.F. Barfuss, I. Chakaberia, A. Ivanov, S. Khalil, M. Makouski, Y. Maravin, L.K. Saini, S. Shrestha, I. Svintradze

Lawrence Livermore National Laboratory, Livermore, USA

J. Gronberg, D. Lange, F. Rebassoo, D. Wright

University of Maryland, College Park, USA

A. Baden, B. Calvert, S.C. Eno, J.A. Gomez, N.J. Hadley, R.G. Kellogg, T. Kolberg, Y. Lu, M. Marionneau, A.C. Mignerey, K. Pedro, A. Skuja, M.B. Tonjes, S.C. Tonwar

Massachusetts Institute of Technology, Cambridge, USA

A. Apyan, R. Barbieri, G. Bauer, W. Busza, I.A. Cali, M. Chan, L. Di Matteo, V. Dutta, G. Gomez Ceballos, M. Goncharov, D. Gulhan, M. Klute, Y.S. Lai, Y.-J. Lee, A. Levin, P.D. Luckey, T. Ma, C. Paus, D. Ralph, C. Roland, G. Roland, G.S.F. Stephans, F. Stöckli, K. Sumorok, D. Velicanu, J. Veverka, B. Wyslouch, M. Yang, M. Zanetti, V. Zhukova

University of Minnesota, Minneapolis, USA

B. Dahmes, A. De Benedetti, A. Gude, S.C. Kao, K. Klapoetke, Y. Kubota, J. Mans, N. Pastika, R. Rusack, A. Singovsky, N. Tambe, J. Turkewitz

University of Mississippi, Oxford, USA

J.G. Acosta, S. Oliveros

University of Nebraska-Lincoln, Lincoln, USA

E. Avdeeva, K. Bloom, S. Bose, D.R. Claes, A. Dominguez, R. Gonzalez Suarez, J. Keller, D. Knowlton, I. Kravchenko, J. Lazo-Flores, S. Malik, F. Meier, G.R. Snow

State University of New York at Buffalo, Buffalo, USA

J. Dolen, A. Godshalk, I. Iashvili, A. Kharchilava, A. Kumar, S. Rappoccio

Northeastern University, Boston, USA

G. Alverson, E. Barberis, D. Baumgartel, M. Chasco, J. Haley, A. Massironi, D.M. Morse, D. Nash, T. Orimoto, D. Trocino, D. Wood, J. Zhang

Northwestern University, Evanston, USA

K.A. Hahn, A. Kubik, N. Mucia, N. Odell, B. Pollack, A. Pozdnyakov, M. Schmitt, S. Stoynev, K. Sung, M. Velasco, S. Won

University of Notre Dame, Notre Dame, USA

A. Brinkerhoff, K.M. Chan, A. Drozdetskiy, M. Hildreth, C. Jessop, D.J. Karmgard, N. Kellams, K. Lannon, W. Luo, S. Lynch, N. Marinelli, T. Pearson, M. Planer, R. Ruchti, N. Valls, M. Wayne, M. Wolf, A. Woodard

The Ohio State University, Columbus, USA

L. Antonelli, J. Brinson, B. Bylsma, L.S. Durkin, S. Flowers, C. Hill, R. Hughes, K. Kotov, T.Y. Ling, D. Puigh, M. Rodenburg, G. Smith, C. Vuosalo, B.L. Winer, H. Wolfe, H.W. Wulsin

Princeton University, Princeton, USA

E. Berry, O. Driga, P. Elmer, P. Hebda, A. Hunt, S.A. Koay, P. Lujan, D. Marlow, T. Medvedeva, M. Mooney, J. Olsen, P. Piroué, X. Quan, H. Saka, D. Stickland², C. Tully, J.S. Werner, S.C. Zenz, A. Zuranski

University of Puerto Rico, Mayaguez, USA

E. Brownson, H. Mendez, J.E. Ramirez Vargas

Purdue University, West Lafayette, USA

E. Alagoz, V.E. Barnes, D. Benedetti, G. Bolla, D. Bortoletto, M. De Mattia, Z. Hu, M.K. Jha, M. Jones, K. Jung, M. Kress, N. Leonardo, D. Lopes Pegna, V. Maroussov, P. Merkel, D.H. Miller, N. Neumeister, B.C. Radburn-Smith, X. Shi, I. Shipsey, D. Silvers, A. Svyatkovskiy, F. Wang, W. Xie, L. Xu, H.D. Yoo, J. Zablocki, Y. Zheng

Purdue University Calumet, Hammond, USA

N. Parashar, J. Stupak

Rice University, Houston, USA

A. Adair, B. Akgun, K.M. Ecklund, F.J.M. Geurts, W. Li, B. Michlin, B.P. Padley, R. Redjimi, J. Roberts, J. Zabel

University of Rochester, Rochester, USA

B. Betchart, A. Bodek, R. Covarelli, P. de Barbaro, R. Demina, Y. Eshaq, T. Ferbel, A. Garcia-Bellido, P. Goldenzweig, J. Han, A. Harel, A. Khukhunaishvili, D.C. Miner, G. Petrillo, D. Vishnevskiy

The Rockefeller University, New York, USA

R. Ciesielski, L. Demortier, K. Goulios, G. Lungu, C. Mesropian

Rutgers, The State University of New Jersey, Piscataway, USA

S. Arora, A. Barker, J.P. Chou, C. Contreras-Campana, E. Contreras-Campana, D. Duggan, D. Ferencek, Y. Gershtein, R. Gray, E. Halkiadakis, D. Hidas, A. Lath, S. Panwalkar, M. Park, R. Patel, V. Rekovic, S. Salur, S. Schnetzer, C. Seitz, S. Somalwar, R. Stone, S. Thomas, P. Thomassen, M. Walker

University of Tennessee, Knoxville, USA

K. Rose, S. Spanier, A. York

Texas A&M University, College Station, USA

O. Bouhali⁵⁴, R. Eusebi, W. Flanagan, J. Gilmore, T. Kamon⁵⁵, V. Khotilovich, V. Krutelyov, R. Montalvo, I. Osipenkov, Y. Pakhotin, A. Perloff, J. Roe, A. Rose, A. Safonov, T. Sakuma, I. Suarez, A. Tatarinov

Texas Tech University, Lubbock, USA

N. Akchurin, C. Cowden, J. Damgov, C. Dragoiu, P.R. Duderu, J. Faulkner, K. Kovitanggoon, S. Kunori, S.W. Lee, T. Libeiro, I. Volobouev

Vanderbilt University, Nashville, USA

E. Appelt, A.G. Delannoy, S. Greene, A. Gurrola, W. Johns, C. Maguire, Y. Mao, A. Melo, M. Sharma, P. Sheldon, B. Snook, S. Tuo, J. Velkovska

University of Virginia, Charlottesville, USA

M.W. Arenton, S. Boutle, B. Cox, B. Francis, J. Goodell, R. Hirosky, A. Ledovskoy, H. Li, C. Lin, C. Neu, J. Wood

Wayne State University, Detroit, USA

S. Gollapinni, R. Harr, P.E. Karchin, C. Kottachchi Kankanamge Don, P. Lamichhane, J. Sturdy

University of Wisconsin, Madison, USA

D.A. Belknap, D. Carlsmith, M. Cepeda, S. Dasu, S. Duric, E. Friis, R. Hall-Wilton, M. Herndon,

A. Hervé, P. Klabbers, A. Lanaro, C. Lazaridis, A. Levine, R. Loveless, A. Mohapatra, I. Ojalvo, T. Perry, G.A. Pierro, G. Polese, I. Ross, T. Sarangi, A. Savin, W.H. Smith, N. Woods

†: Deceased

- 1: Also at Vienna University of Technology, Vienna, Austria
- 2: Also at CERN, European Organization for Nuclear Research, Geneva, Switzerland
- 3: Also at Institut Pluridisciplinaire Hubert Curien, Université de Strasbourg, Université de Haute Alsace Mulhouse, CNRS/IN2P3, Strasbourg, France
- 4: Also at National Institute of Chemical Physics and Biophysics, Tallinn, Estonia
- 5: Also at Skobeltsyn Institute of Nuclear Physics, Lomonosov Moscow State University, Moscow, Russia
- 6: Also at Universidade Estadual de Campinas, Campinas, Brazil
- 7: Also at California Institute of Technology, Pasadena, USA
- 8: Also at Laboratoire Leprince-Ringuet, Ecole Polytechnique, IN2P3-CNRS, Palaiseau, France
- 9: Also at Joint Institute for Nuclear Research, Dubna, Russia
- 10: Also at Suez University, Suez, Egypt
- 11: Also at Cairo University, Cairo, Egypt
- 12: Also at Fayoum University, El-Fayoum, Egypt
- 13: Also at British University in Egypt, Cairo, Egypt
- 14: Now at Ain Shams University, Cairo, Egypt
- 15: Also at Université de Haute Alsace, Mulhouse, France
- 16: Also at Brandenburg University of Technology, Cottbus, Germany
- 17: Also at The University of Kansas, Lawrence, USA
- 18: Also at Institute of Nuclear Research ATOMKI, Debrecen, Hungary
- 19: Also at Eötvös Loránd University, Budapest, Hungary
- 20: Also at University of Debrecen, Debrecen, Hungary
- 21: Now at King Abdulaziz University, Jeddah, Saudi Arabia
- 22: Also at University of Visva-Bharati, Santiniketan, India
- 23: Also at University of Ruhuna, Matara, Sri Lanka
- 24: Also at Isfahan University of Technology, Isfahan, Iran
- 25: Also at Sharif University of Technology, Tehran, Iran
- 26: Also at Plasma Physics Research Center, Science and Research Branch, Islamic Azad University, Tehran, Iran
- 27: Also at Università degli Studi di Siena, Siena, Italy
- 28: Also at Centre National de la Recherche Scientifique (CNRS) - IN2P3, Paris, France
- 29: Also at Purdue University, West Lafayette, USA
- 30: Also at Universidad Michoacana de San Nicolas de Hidalgo, Morelia, Mexico
- 31: Also at Institute for Nuclear Research, Moscow, Russia
- 32: Also at St. Petersburg State Polytechnical University, St. Petersburg, Russia
- 33: Also at Faculty of Physics, University of Belgrade, Belgrade, Serbia
- 34: Also at Facoltà Ingegneria, Università di Roma, Roma, Italy
- 35: Also at Scuola Normale e Sezione dell'INFN, Pisa, Italy
- 36: Also at University of Athens, Athens, Greece
- 37: Also at Paul Scherrer Institut, Villigen, Switzerland
- 38: Also at Institute for Theoretical and Experimental Physics, Moscow, Russia
- 39: Also at Albert Einstein Center for Fundamental Physics, Bern, Switzerland
- 40: Also at Gaziosmanpasa University, Tokat, Turkey
- 41: Also at Adiyaman University, Adiyaman, Turkey
- 42: Also at Cag University, Mersin, Turkey
- 43: Also at Mersin University, Mersin, Turkey

- 44: Also at Izmir Institute of Technology, Izmir, Turkey
- 45: Also at Ozyegin University, Istanbul, Turkey
- 46: Also at Kafkas University, Kars, Turkey
- 47: Also at Mimar Sinan University, Istanbul, Istanbul, Turkey
- 48: Also at Rutherford Appleton Laboratory, Didcot, United Kingdom
- 49: Also at School of Physics and Astronomy, University of Southampton, Southampton, United Kingdom
- 50: Also at University of Belgrade, Faculty of Physics and Vinca Institute of Nuclear Sciences, Belgrade, Serbia
- 51: Also at Argonne National Laboratory, Argonne, USA
- 52: Also at Erzincan University, Erzincan, Turkey
- 53: Also at Yildiz Technical University, Istanbul, Turkey
- 54: Also at Texas A&M University at Qatar, Doha, Qatar
- 55: Also at Kyungpook National University, Daegu, Korea